UNIVERSITY OF TROMSØ UIT

FACULTY OF SCIENCE AND TECHNOLOGY
DEPARTMENT OF PHYSICS AND TECHNOLOGY

Wet snow detection by C-band SAR in avalanche forecasting

Ingrid S. Hopsø

EOM-3901 Master's Thesis in Energy, Climate and Environment

December 2013

Abstract

Avalanches usually occur in steep, snow-covered mountain sides under special conditions. The stability of the snowpack depends, among other things, on the melting and freezing of the snowpack. If a snow covered area has not undergone a melt/freeze-process, it could potentially be unstable due to depth hoar or buried layers of frost, and therefore pose an avalanche risk if the area is located at a steep enough mountain side. Additionally, when the snow has been wet early in the winter, it can form a frozen crust later. This crust could constitute the sliding layer when large amounts of new snow accumulates, but the same crust could also contribute to forming unstable layers in the snow by acting as a lid and trapping water vapor from the bottom of the snowpack. These mechanisms are important for avalanche buildup, and improved information from remote sensing could be valuable for avalanche forecasting.

C-band SAR can be used to detect wet snow. Time series of maps with detected wet snow can be made by combining SAR data from periods of melting snow with reference SAR data from a period of dry snow. Since wet snow absorbs radar waves, one can detect wet snow by a scattering coefficient reduction of -3dB or more.

A pattern was found in four of the seven avalanche events studied, which might be used to predict future avalanches.

Forord

Masteroppgaveskrivingen har vært en interessant og lærerik opplevelse. Jeg har lært mye om SAR og snøskred, men jeg har lært minst like mye om Matlab-programmering (det ligger tross alt 31 sider med Matlab-kode bak figurene i oppgaven min) og hvordan man skriver vitenskapelige tekster.

Jeg har først og fremst lyst til å takke veilederen min, Eirik Malnes, som har vært veldig hjelpsom og tålmodig. Han har funnet seg i sure miner og sent innleverte oppgaveutkast uten å klage, og han har kommet med konstruktive tilbakemeldinger som har gitt meg mye hjelp.

Jeg har også lyst til å takke alle de som orker å stille spørsmål på internettforum, sånn at slike som jeg kan søke opp svarene de har fått. Til slutt har jeg har lyst til å takke vennene mine som har foret meg med kaffe og mosjonert meg ved behov. Dere er gode å ha!

Ingrid Hopsø
Tromsø, Desember 2013

Cover photo: Thomas Holm Osbakk

Contents

Chapter 1

Introduction

Avalanches ruin road infrastructure, buildings, power lines, and, as the interest for more extreme outdoor activities and tourism have become more popular, kill an increasing number of people each year. There is no reason to believe that the costs of avalanches, both financially and socially, will be reduced in the future, so there is an increasing need for more effective and better avalanche forecasting than we have today.

Avalanche forecasting in Norway relies on temperature data, precipitation data, and wind data, which is sampled at a few weather stations and then approximated for the areas of interest, and observations made by certified observers in the field. While the data gathered by certified observers is probably better than computer generated data, the observers can only cover a very small area and it is time-consuming for the observers to get around to different locations. This poses a problem as wind and other weather conditions can change the snow on a small scale, making the snow structure on one side of a mountain completely different from the snow structure on the other side of the same mountain. A snow monitoring sensor that can operate on larger scales than the observers can would obviously be useful when it comes to avalanche forecasting.

In 1952 W.A. Cumming investigated the effects of microwave radiation with a wavelength of 3.2 cm on snow. He found that the loss tangent in wet snow was higher than the loss tangent in dry snow [8]. Stiles and Ulaby continued this research and found that the backscattering coefficient decreased with increasing liquid water content in their studies from 1980, where they tested the active and passive microwave response to wet snow [33]. Rott found in 1984, that the ideal frequencies for monitoring snow with active microwave

sensors were X- and C-band, due to the difference in backscattering between wet snow and snow-free ground at these frequencies. He also found that the differences diminished for lower frequencies [27]. Koskinen et al. (1997) showed that SAR could be used to make snowmelt maps, even though SAR cannot distinguish between dry snow and snow-free ground [17]. In 2000, Nagler and Rott developed an algorithm for mapping wet snow using the change in backscatter between a wet snow image and a dry snow or snow-free image. They found that a threshold of -3 dB can be used to differentiate wet snow from other surfaces [21].

This research shows that SAR is a useful sensor when to remote sensing of snow. SAR can provide detailed geographical info that is not approximated, it covers greater areas than observers, and SAR can give almost daily updates of the areas it covers. SAR also has the advantage of being weather and light independent, so it doesn't run into the same problems with clouds and lack of daylight as imaging spectrometers do. It is possible to use SAR to observe a snowpack from the beginning of the snow season to the end of the season, or until an avalanche is released. Timeseries of SAR-data could provide valuable information on how the snowpack behaves under various weather conditions can reveal how the different weather conditions affect the snow stability in an avalanche area.

With SAR data I can form wet snow maps which help me investigate the effects of early and mid-winter snowmelt on the snowpack. Can warm weather during the winter season contribute to stabilization of the snowpack as the melting removes unstable layers in the snow, or, at the other end of the spectrum, can it destabilize the snow by forming ice crusts that will become unstable layers later in the season? I also want to look at different methods for making reference images that are used to make wet snow maps, and try to find the preferred method to use later in my wet snow detection algorithm.

Firstly, the thesis will go through some background theory to improve the understanding of how snow behaves, both during a winter season, and as a target object for a radar. Chapter 2 covers snow as a medium in a remote sensing perspective, while chapter 3 focuses on focuses on the radar response from snow. Avalanche theory is reviewed in chapter 4, ending with a short resume of the operational avalanche forecasting in Norway today. Chapter 5 discloses the algorithm used to classify wet snow in SAR images, as well as the differences between the three reference image methods used in the wet snow classification. Results from the wet snow classification algorithm and the different reference methods are laid out in chapter 6, and then discussed in chapter 7. A conclusion of the thesis and a discussion concerning future

work on the field of the thesis is given in chapter 8.

1.1 Abbreviations and Acronyms

SAR	Synthetic Aperture Radar
SCAW	Snow Cover Area Wet
DEM	Digital Elevation Model
Envisat	Environmental Satellite
ESA	European Space Agency
Norut	Northern Research Institute, Norway
SWE	Snow Water Equivalent
ASAR	Advanced Synthetic Aperture Radar
NVE	Norwegian Water Resources and Energy Directorate
CoReH2O	Cold Regions Hydrology high-resolution Observatory
Met.no	Norwegian Meteorological Institute

Chapter 2

Snow as a medium

Snow is an interesting material to study as it can consists of ice, air, and liquid water, where the amount of each of the components change with changes in external factors, like air temperature, precipitation, solar temperature, etc. In this section we will discuss the macroscopic properties of snow such as density, depth, and snow water equivalent (SWE), before we discuss how various sensors utilize electromagnetic attributes of snow to measure the macroscopic properties.

2.1 Density and depth

An important parameter of snow is its density. Since snow is a mix of air, ice, water and micro particles, the size of ice crystals and amount of air and water in the snowpack affect the density of the pack. The density of snow usually lies between 200-600 kgm^{-3}, but it could be as low as 10 kgm^{-3} under special conditions, like freshly fallen powder snow [25]. The snowpack will settle over time due to metamorphism of the snowflakes that reduces their surface area and make the bonds between the grains stronger [19]. The speed of the metamorphism is a product of wind and temperature changes, among others. As wind and temperature is important for the settling process, the density will vary spatially over small areas, and can be hard to model.

Snow depth is the height of the snow cover from the ground and to the surface of the cover. As with snow density, the snow depth will follow the settling process of the snowpack. This means that the depth will vary spatially. For snow depth, the variations are mostly due to wind transport of snow and

micro topography including vegetation, and to a lesser extent temperature changes [19].

Knowledge about the snow cover density and depth can be used to estimate the snow cover's water content.

2.2 Snow Water Equivalent

The amount of water in the snowpack is called snow wetness, and is the amount of water by volume in percent of a unit volume of snow. At temperatures below 0°C, it is not likely to find liquid water in the snowpack, since the water will be frozen. The snowpack is then classified as dry snow. At temperatures of 0 degrees and above, liquid water can be found within the snowpack. The snow water equivalent (SWE) is a measure of the amount of water within a unit area of the snowpack, and is given by

$$d_w = \frac{1}{\rho_w} \int_0^d \rho_s(z)\,\mathrm{d}z \tag{2.1}$$

where ρ_w is the density of water, $\mathrm{d}z$ is a unit length of depth d of the snowpack, and $\rho_s(z)$ is the density of the snowpack as a function of depth [25]. The density of the snowpack is seldom uniform due to different layers in the pack, which makes ρ_s hard to estimate.

Knowledge about SWE is important for, e.g., hydro power plant companies which want to calculate the probable runoff from the seasonal snow cover, or for countries where snow-melt contributes in a large scale to the national water supply.

2.3 Grain size

Snow crystals are created in clouds where the temperature is below 0°C. The crystals come in all shapes and sizes, and as they fall towards the ground, they change depending on temperature and humidity in the atmosphere. Grains normally vary between 0.1 to 4 mm, measured as the mean radius of the grain [19]. On the ground, the crystals go through a metamorphism that alters their structure, size, and bond strength.

In remote sensing, grain size refers to the optical properties and size of the surface and near-surface grains, and can be measured by relating snow surface reflectance to changes in grain size [23]. Knowledge about surface grain size is important in avalanche forecasting, which we will see later on in this chapter.

2.4 Optical measurements of snow

Optical sensors measure the reflected energy from Earth's surface. They usually operate in the visible, near-infrared, and infrared spectrum. Images taken in the visible or infrared range provide relatively high resolution data with global coverage [26]. In the visible region, snow is characterized by a large albedo, or reflectance, but in the infrared region the albedo of snow is low, since snow absorbs almost all of the incoming infrared radiation. This unique feature of snow is used in mapping snow covered ground with optical instruments. Solberg et al. (2009) found that optical sensors can detect changes in snow grain size, measure snow surface temperature and snow surface wetness.

Optical sensors are used to provide maps of snow cover, as they provide images with high resolution and it is relatively easy to detect snow in the images. One disadvantage with using optical sensors is that they are dependent on illumination from the Sun. This means that the sensors cannot operate during night time or when it is cloudy. Other disadvantages include underestimating snow cover when measuring in areas with vegetation, and problems measuring areas where the snow cover is patchy [26].

Optical sensors available today are, amongst other, the MODIS (Moderate Resolution Imaging Spectroradiometer) and the Landsat Thematic Mapper.

2.5 Passive microwaves measurements of snow

Passive microwave instruments measures the microwave energy sent out from Earth, where the microwave region is defined to range from around 1 mm to 30 cm, or 1-300 GHz [13]. Dry snow will scatter the microwave energy emitted from the ground underneath the snow cover, and thus it is possible to measure a drop in the emitted microwave energy when measuring from snow free land to snow covered land [1]. Microwave sensors have the advantage of being light independent, and can therefore operate both night and day. Microwaves are

not affected by most clouds, which is a big advantage when monitoring snow, since snow and cloud cover is closely connected. Passive microwave sensors have to operate on a large scale since the microwave emissions from Earth are so small. This gives a resolution of approximately 25 km [23]. Another problem is that wet snow emits almost the same amount of microwave energy as snow-free ground [23], which means that passive microwave sensors will underestimate the total snow covered area during snowmelt.

Passive microwave sensors operating today are, amongst other, the SSMI/I (Special Sensor Microwave Imager).

2.6 SAR measurements of snow

SAR is an active sensor which sends out signals in the microwave region and measures the backscattered signal. Depending on the condition of the snow cover, the signal is scattered by the surface, ice particles in the volume, and from the ground underneath the snow cover. When the snow is dry, dielectric losses in the snowpack are low, which means that most of the electromagnetic wave energy is preserved during propagation through the snow layer, and scattering from the ground dominates. When the snow is wet, the dielectric losses in the snowpack increases and scattering from the surface dominates [28].

Name	Width (cm)	Central value	Frequency (GHz)
Ka	0.75-1.10		
K	1.10-1.67	1.0	10.90-36.00
Ku	1.67-2.40		
X	2.40-3.75	3.0	5.75-10.90
C	3.75-7.50	5.6	3.90-5.75
S	7.50-15.00	10.0	1.55-3.90
L	15.00-30.00	23.00	0.39-1.55
P	30.00-100.00	70.00	> 0.39

Table 2.1: Bands frequently used in microwave remote sensing. *Rendered from [6].*

SAR has the advantage of being light-independent and cloud penetrating, and it provides images with a spatial resolution on scales from 1m to 1km. Radarsat-2 (used in this paper), has a spatial resolution of 30 m[23]. The

SARs used in this study operates at C-band frequencies, which works when measuring wet snow, but does not work well when measuring dry snow, since the penetration depth of electromagnetic waves at C-band frequencies in snow is approximately 20 m. [18]. Dry snow sensing with a combination of Ku-band and X-band have proven to be sensitive to dry snow. For shallow snowpacks, bacscattering at X-band frequencies is mostly dependent of scattering from the ground surface beneath the snow layer. For deeper snowpacks and/or larger snow grains, volume scattering from the snow layer becomes more important at X-band frequencies. At Ku-band frequencies backscatter from the snow is more dependent on volume scattering, even for shallow snowpacks [7]. An overview of different bands frequently used in microwave remote sensing can be found in table 2.1.

A list of active and earlier SAR are presented in table 2.2. In this paper, data from Radarsat-2 and Envisat ASAR (Advanced Synthetic Aperture Radar) will be used. The Envisat ASAR was launched in March 2002 by the European Space Agency (ESA). The Envisat is a polar-orbiting satellite, designed to measure atmosphere, ocean, land, and ice. In April 2012, ESA lost contact with the satellite, and the mission was declared ended in May 2012 [12]. The ASAR operates at C-band. RADARSAT-2 followed the RADARSAT-1 system, and was launched in 2007, and is planned to operate for seven years [29].

Sensor	Frequency (GHz)	Polarization	Incidence in degree	Pixel resolution (m)	Available time fram
ERS-1/2	5.3	VV	Fixed at 23°	3.8-12.5	Since 1991/ 1995
ASAR	5.33	Dual-polarization	Varying with mode	3.8-150	Since 2002
RADARSAT-1	5.3	HH	Varying with mode	10-100	Since 1997
SIR-C/X-SAR	1.25 and 5.3/9.6	Fully polarimetric/VV	Varying with data takes	6-27	April and Oct., 1994
JERS-1	1.27	HH	Fixed at 35°	18	Since 1994-1997
PALSAR	1.27	Fully polarimetric, dual-polarization and HH	Varying with mode	10-100	Since Dec. 2005
RADARSAT-2	5.3	Fully polarimetric, dual-polarization and HH	Varying with mode	3-100	2007
TerraSAR-X	9.6	VV or dual-polarization	Varying with mode	1-16	2007

Table 2.2: Characteristics of spaceborn SARs. *Rendered from [29]*

Chapter 3

Remote sensing of snow using SAR

SAR is a side-looking radar that sends out a signal pulse from an antenna with a side-looking orientation. The radar scans the terrain as it moves forward, so the antenna beam in along-track direction is narrow. The signal reflections of the terrain results in a two-dimensional image, where one dimension is the direction perpendicular to the radar motion, the slant-range, and the other dimension is the azimuthal, or along-track, direction (see Figure 3.1).

A SAR operates in the microwave region and is its own source of illumination, since it is an active sensor. This means that a SAR can operate independently of the time of day and during the polar night. Microwave radiation can penetrate clouds, which gives the radar an advantage over visible and infrared sensors. Radiation in the microwave region can also give us information about the terrain that we can not get from visible and infrared sensors.

A SAR image is the result of the scattering of the radar pulse by the surface and the sub-surface of the area illuminated by the radar. Radars can operate at different wavelengths, which is shown in table 2.1. The longer wavelengths, P and L band, give a strong return for larger surface features, and they can penetrate soil, canopies, and snow to a certain depth. Shorter wavelengths, C and X band, give a strong return for smaller objects. These wavelengths do not penetrate as deep as the longer wavelengths mentioned earlier [3]. Different combinations of the polarization of the transmitted signal and the returned signal can also contribute to further characterization of the surface terrain. Same polarization, horizontal transmitted and horizontal received (HH) or vertical transmitted and vertical received (VV), gives a

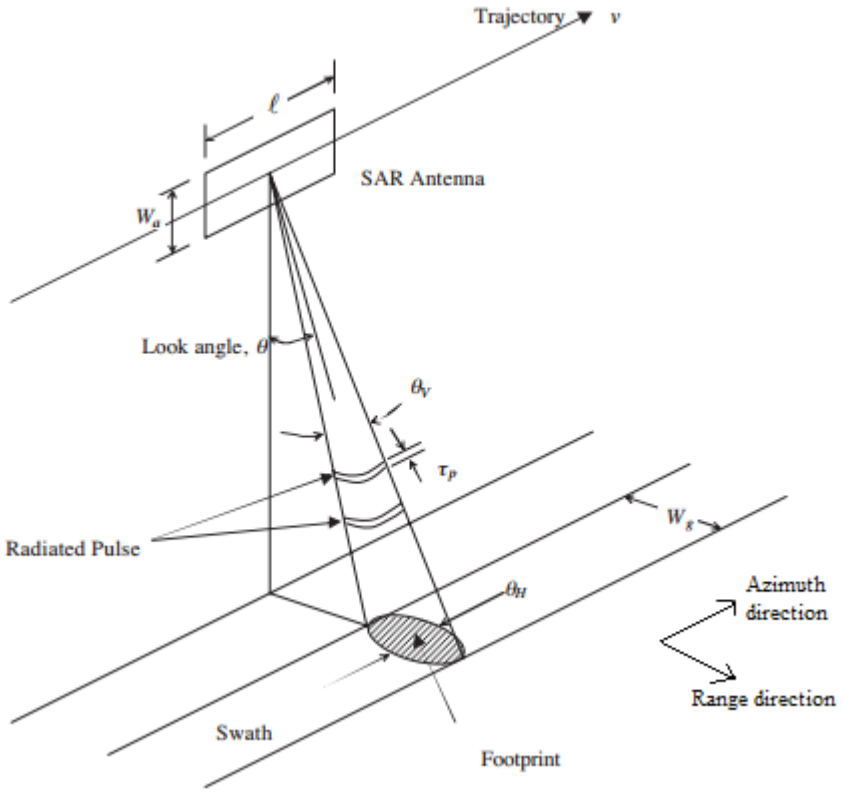

Figure 3.1: Imaging geometry of a SAR. *Image borrowed from [Chan and Koo, 2008].*

stronger signal return for objects that are orientated in the same direction as the incoming radiation. Cross-polarization, HV or VH, is more sensitive to areas with multiple scatters and multiple bounces, such as ground to building reflections [3].

The radar equation for a SAR system is

$$P_r = \frac{P_t G^2 \lambda^2 \sigma}{(4\pi)^3 R^4} \tag{3.1}$$

where P_r is the power received by the antenna, P_t is the power transmitted, G is the antenna gain, R is the distance from radar to the target, λ is the wavelength of the signal, and σ is the radar cross-section [5]. The radar cross section is a measurement of how effectively the observed medium scatters the incoming radar waves. It is a function of, from the apperatus' side, frequency, polarization, radar geometry, and the target area, but it is also dependent

on the dielectric properties and geometry of the target. The cross section is normalized by dividing the backscatter coefficient by the illuminated area [29]. Later in this section we will look at the radar cross section of snow.

3.1 Backscatter model

According to the $CoReH_2O$-report, total backscatter from snow is the sum of these contributions:

$$\sigma^t_{pq} = \sigma^{as}_{pq} + \sigma^{v}_{pq} + \sigma^{gv}_{pq} + \sigma^{g'}_{pq} \tag{3.2}$$

where the subscript pq represent transmit and receive polarization, σ^{as} is the scattering at the air/snow boundary, σ^{v} is the direct volume scattering term, σ^{gv} is the scattering at the ground/volume and volume/ground boundary, and $\sigma^{g'}$ represents the scattering from the ground surface after transmission through the snow (see Figure 3.2). In the following sections we will discuss the various scattering terms in Equation (3.2) but first we need to discuss the dielectric properties of snow.

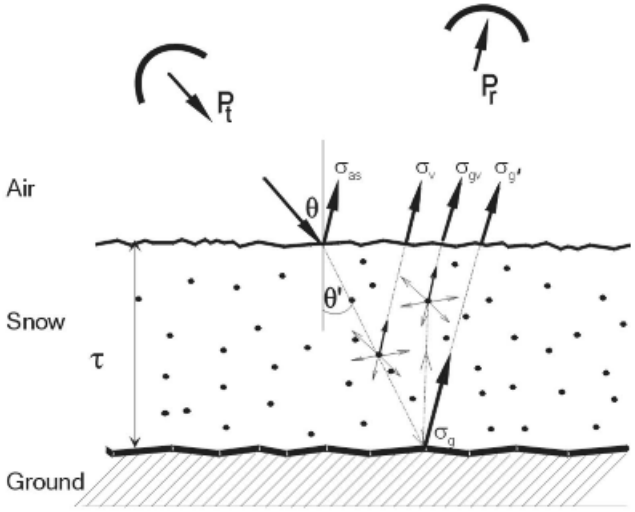

Figure 3.2: Scattering mechanisms in the snowpack. P_t is the transmitted radar signal, P_r is the received radar signal, θ is the incidence angle, θ' is the refractive angle, and τ is the depth of the snowpack. *Image borrowed from the $CoReH_2O$-project report.*

3.2 Permittivity

Dielectric properties tells us something about how a material reacts to an electric field [13]. The electromagnetic properties of a material is defined by the magnetic permeability, μ, and the relative complex dielectric constant, also known as complex relative permittivity, ϵ, of the material. For most naural materials, the magnetic permeability of the material equals the magnetic permeability of free space, μ_0 [34]. This means that the defining factor for the electromagnetic propagation is the dielectric constant, which is written as

$$\epsilon = \epsilon' - \jmath\epsilon'' \tag{3.3}$$

The dielectric constant ϵ of a medium is made up of a real component, ϵ', which accounts for the propagation characteristics of an electromagnetic wave in the medium, and an imaginary component, ϵ'', which accounts for the losses from damping in the medium [13]. From an electromagnetic perspective, snow is a dielectric mixture of air, ice particle, and, under certain conditions, liquid water [34]. For dry snow, the dielectric constant varies between $\epsilon = 1$ (for air) and $\epsilon = 3.2$ (for ice), depending on the snow structure and snow temperature [13], [33]. Water has a dielectric constant of approximately $35\epsilon_0$ (ϵ_0 is the permittivity of vacuum) for low frequency radiation (20 GHz). This means that the amount of liquid water in the snowpack will greatly affect the dielectric properties of the snow and therefore also affect the backscattered radar signal in the microwave region [33, 13].

3.3 Penetration depth

"The penetration depth in a medium is defined as the depth at which the average power of a wave traveling downward in the medium is equal to 1/e of the power at a point just beneath the surface of the medium."[34]. The electromagnetic penetration depth is denoted by δ_p, and is given as

$$\delta_p = 1/\kappa_e \tag{3.4}$$

where κ_e is known as the extinction coefficient which is the sum of a scattering coefficient, κ_s, and an absorption coefficient, κ_a. The scattering coefficient is usually ignored when the snow is wet, since it is considerably smaller than the absorption coefficient. This also holds for dry snow for frequencies lower than 5 GHz, which means that the penetration depth can be written as

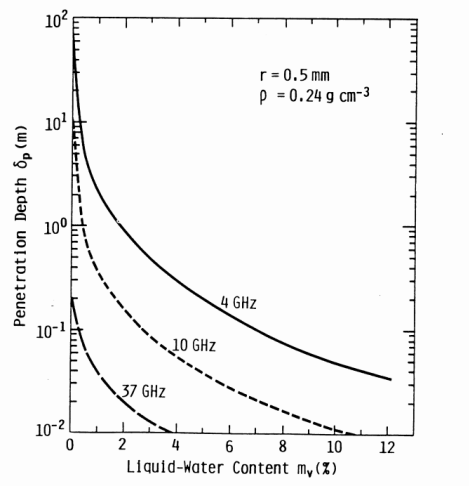

Figure 3.3: Penetration depth changes with the amount of liquid water content at 4 GHz, 10 GHz, and 37 GHz. The density of the snow is 0.24 g cm^{-3} and the radius of the snow crystals is 0.5 mm. *Image borrowed from [14].*

$$\delta_p = 1/\kappa_a \tag{3.5}$$

The absorption coefficient is defined as

$$\kappa_a = \frac{\lambda_r}{4\pi}\left(\frac{\epsilon'}{2}\left[\left[1+\left(\frac{\epsilon''}{\epsilon'}\right)^2\right]^{\frac{1}{2}}-1\right]\right)^{\frac{1}{2}} \tag{3.6}$$

where λ_r is the wavelength in cm, and the penetration depth becomes

$$\delta_p = \frac{4\pi}{\lambda_r}\left(\frac{\epsilon'}{2}\left[\left[1+\left(\frac{\epsilon''}{\epsilon'}\right)^2\right]^{\frac{1}{2}}-1\right]\right)^{-\frac{1}{2}} [\text{cm}] \tag{3.7}$$

If $\frac{\epsilon''}{\epsilon'} \ll 1$, Equation (3.7) becomes

$$\delta_p \approx \frac{\lambda_r\sqrt{\epsilon'}}{2\pi\epsilon''} \tag{3.8}$$

which can be used for dry snow and wet snow where the liquid water volume content is less than 2% [2, 34]. Figure 3.3 shows the relationship between penetration depth and liquid water content for frequencies in the microwave range.

3.4 Backscatter from dry snow

Dry snow is an inhomogeneous medium consisting of ice particles in an air medium. According to Hallikainen et al. (1986), absorption losses as dominant for dry snow where the ice particles are assumed identical and with a radius of 0.5 mm, and interactions between the particles are ignored, for frequencies lower than 14 GHz. At frequencies higher than 14 GHz, volume scattering losses are dominant. The dielectric constant of dry snow increases almost linearly with increasing snow density [14].

3.5 Backscatter from wet snow

Wet snow is a medium consisting of ice particles in an air-water mixture. The presence of water increases the dielectric constant, and the penetration depth for wet snow with a water content of 2-4% is usually in the order of one wavelength only [28]. This means that the backscattering of wet snow is mainly due to surface scattering at the air/snow boundary, which implies that surface roughness of the wet snow layer determines the amount of scattering at this interface. According to Nagler and Rott (2000), wet snow will give a difference in backscattering coefficient of -3dB or less when compared to backscattering coefficient from dry snow or snow-free ground. Here wet snow is assumed to be snow with a liquid water volume content of 4% or more [21]. For liquid water content above 1%, volume scattering losses are negligible, and absorption due to the air-water mixture dominates for frequencies ranging from 1 to 40 GHz [14]. According to Rott and Matzler (1987), a SAR operating in the X-band ($\lambda = 3$ cm) would be the best option for wet snow detection, but a C-band SAR could also be used.

Chapter 4

Avalanches

The physics of avalanches is complex. There are so many variables to take into account that simplifications are a necessity. The lack of good physical models of avalanche release mechanisms and the contributing factors to avalanches make avalanche prediction very difficult.

This paper will focus mostly on remote sensing of wet snow, so only avalanche theory related to wet snow will be discussed. The hypothesis is that a melt/freeze-process early in the winter season can either remove unstable layers or produce a layer of metamorphed snow that can become a sliding bed for avalanches later in the season.

4.1 Metamorphism of snow

When new snow falls to the ground, it immediately starts to change shape and structure. Newly fallen snow is often light, fluffy and uncohesive. In cold, still weather, newly fallen snow can contain up to 99% air and only 1% ice, and the snow's density can be as low as 10kg/m^3. Normally, the density of new snow is approximately 100kg/m^3, which is about 10% of the density of water [16]. The fresh snow will quickly be affected by the weather. These changes of the snowpack are known as metamorphism. There are three main types of metamorphisms in the snowpack: equitemperature metamorphism, temperature gradient metamorphism, and melt metamorphism.

4.2 Equitemperature metamorphism

Equitemperature metamorphism occurs when all the snow in the snowpack holds the same temperature. This metamorphism creates rounder grains, and smaller grains tend to melt, while bigger grains tend to get bigger. The process is affected by temperature, and if the snow is close to 0°C, changes in grain structure could take only a few hours. If the snow has a temperature of −5°C, changes can take up to a couple of weeks [16]. This is an example of how warm periods can help stabilize the snow, as rounder grains tend to form stronger bonds between themselves than other types of snow crystals.

4.3 Temperature gradient metamorphism

Temperature gradient metamorphism occurs when there is a temperature difference from the top of the snow cover to the bottom of it. In early winter the ground usually is warmer than the air above the snow cover, so when snow falls upon the warm ground, we get a temperature gradient within the snow. If the gradient is steep enough (10°C/m), the snow undergoes temperature gradient metamorphism [16]. Depth hoar is created at the bottom of the snowpack if the temperature gradient exceeds 25°C/m [19]. Depth hoar is large, faceted snow crystals, and is known as an unstable layer.

4.4 Melt metamorphism

Melt metamorphism occurs if the temperature of the snow passes 0°C. Water vapor due to melting of the snow will produce a film of water over the crystals' surface which bonds the crystal together with the surface tension of water. This force is strongest when the water content of snow is below 4 % [16]. If the melting continues, free water will appear in the snowpack. The speed of the melt process increases as more water melts, since water has higher heat conductivity than snow, which contains mostly insulating air pockets. Free water will break up the structure of the snow grains and create rounder, larger grains. Smaller grains will melt. After a while the bonds between the snow grains will melt, and we get uncohesive snow, also called "rotten snow" [16].

With melting over a longer period of time, drainage channels in the snow will develop, and the snow will settle and become stable. Melting of snow can

have a positive effect regarding avalanche danger, where the surface tension in the water film bonds the snow grains together, or it can have a negative effect, where melting causes increased creep in snowpack on slopes, which increases the tension within the pack.

4.5 Layering of snow

Temperature, wind speed and direction, and snowfall intensity determines the speed of snow metamorphism, so variations in these parameters will produce variations in the structure of the snow. This means that when new snow falls on top of the metamorphed snow, the snowpack becomes layered. Layers in snow are areas with a wide extent in the horizontal plane, but small extent in the vertical plane, where density, grain size, grain types, bond strength between crystals, or water content, differ from the layer above and beneath. Weak layers can consist of faceted snow, formed within or on top of the snowpack due to temperature differences, frost (or hoar), hail (frozen water droplets), or almost any kind of uncohesive snow [35]. Weak layers in the snowpack are the basis for many avalanches.

4.6 Melting/freezing

If the temperature falls beneath 0°C after a period where the snowpack has undergone a melt metamorphism, the snow will freeze and form a crust. This crust consists of strongly bonded snow crystals. Crusts formed this way can reduce the avalanche risk, as the crust is able to distribute pressure from, e.g., a skier or a sudden snow fall.

On the other hand, crusts like these can also increase the avalanche risk if snow on top of the crust is unable to bond with the crust, thus making the snowpack unstable. The crust can also destabilize the snow in another way, by forming depth hoar, which is large, faceted crystals at the bottom of the snowpack. The crust acts as a lid, and can create a temperature gradient from the ground and up to the crust, which, as mentioned in an earlier section, is able to transform the snow close to the ground into an unstable layer.

Temperatures above 0°C over a long period, followed by a long period of cold temperatures can make the whole snowpack isotropic, thus removing

the layering of the pack because the free water in the snow dissolves bonds and changes the crystal structure. This usually happens in springtime.

4.7 Slab avalanches

A strong layer over a weak layer is called a slab. Wind will redeposit and pack the snow, making slabs, which are relative harder, more cohesive snow than the layer underneath [35]. If a weak layer collapses and the slab starts sliding on the bed surface, we have a slab avalanche. Layers of, e.g., depth hoar can collapse if the weight of the snowpack suddenly increases, as with a new snow fall or if a skier passes over the area.

Slab avalanches are the most dangerous type of avalanches, and nearly all avalanche accidents are due to slab avalanches [16].

4.8 Slush avalanches

Another type of avalanches that are affected by melting of snow is wet snow avalanches, and, if the snow is fully saturated, slush avalanches. Wet avalanches behave in a different way than dry avalanches, and are triggered differently. Dry avalanches, like slab avalanches, are triggered by adding weight, or stress, to the snowpack, while wet avalanches are triggered by decreasing the strength of the weak layers in the snowpack [35].

In very wet snow, the liquid water in the snowpack dissolves the bonds between the crystals, and forms its own bonds between them due to the surface tension of water. This means that the snowpack is very unstable, and can slide on its own without any extra stress added. Luckily, the snow stabilizes quickly, as drainage channels are formed within the pack and drains the snow. After a couple of days of melting, the snow will most likely be homogenous, or it will already have fractured and slid [35].

4.9 Loose snow avalanches

Loose snow avalanches usually release in freshly fallen, dry snow or in wet snow. They occure when the gravity pull on the snow crystal exceeds the friction between them. Newly formed snow crystals start of as a complex

structure with a lot of branches, keeping the cohesion between the crystals high in the snowpack. But after the crystals have gone through one or more of the metamorphisms mentioned in earlier sections, they loose their complex structure and branches, and the friction and cohesion beween the crystals decreases [16].

Loose snow avalanches do not normally pose a serious risk for the skiers who release them, as the snow is uncohesive and will only release underneath the skier, unlike a slab avalanche, which can crack up above the skier and far out to the sides due to the tension in the cohesive slab [16].

4.10 Avalanche forecasting in Norway today

For the last two winters, Norway has had a regional avalanche forecast, found at *www.varsom.no*. This site is a cooperation between NVE and the Norwegian Meteorological Institute (met.no). The forecasts are based on observations made by both certified avalanche observers from NVE and volunteers, and on meteorological data provided by NMI. *www.varsom.no* uses a five-step risk model to report avalanche danger, where level 1 is little to no risk of avalanches and level 5 is extreme high risk of avalanches. The forecast does not cover all of Norway, and the areas that are not covered, only get avalanche forecasts if the risk level reaches 4 or 5 [24].

Chapter 5

Method for detection of wet snow

5.1 Test site

The test site is located in the Tromsø region from Kvaløya in the west to Kåfjord in the east. A map of the area is shown in Figure 5.1. The area is found in the north of Norway, a region known for long winters and harsh weather. It is an area close to the Atlantic Ocean and the Gulf stream, which gives it a maritime climate and relatively mild winters with large amounts of snow. The terrain consists of mountains, valleys, fjords, and some smaller towns and cities. It is a well-known skiing area, but it is also an area that is known for avalanches, which makes it suitable as a test site for this project.

5.2 Avalanche sites

Four areas within the test site have been chosen to be examined closer due to larger avalanche accidents happening there sometimes between 2005 and today. The areas are Kroken (highest point at 626 m.a.s.l.), an alpine center close to Tromsø city, Middagstinden (1006 m.a.s.l.), a mountain located on Kvaløya, Langfjellaksla (765 m.a.s.l.), also a mountain on Kvaløya, and Sorbmegaisa (1288 m.a.s.l.), a mountain in Kåfjorden.

On February 19th, 2006, a party of skiers was riding down one side of Middagstinden, a mountain north of Kattfjordeidet on Kvaløya. One skier was

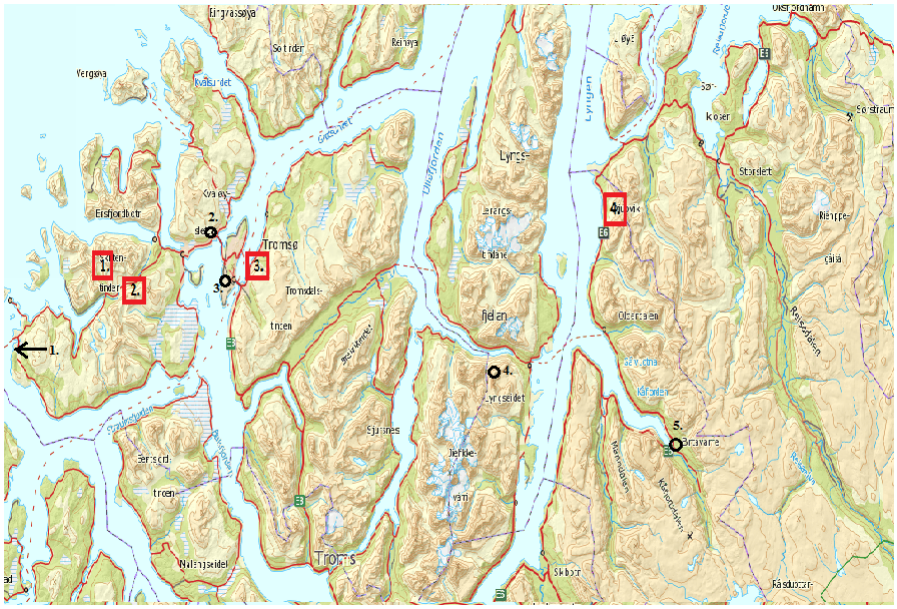

Figure 5.1: Map of the test site with the avalanche areas marked by red squares. 1. is Middagstinden, 2. is Langfjellaksla, 3. is Kroken Alpine Center, and 4. is Sorbmegaisa. The black circles marks the position of the five weather stations, where 1. is Hekkingen fyr, 2. is Kvaløysletta, 3. is Holt, 4. is Gjerdvassbu, and 5. is Skibotn II.

taken by an avalanche, but managed to avoid being completely buried. On February 18th, 2012, four men were taken by an avalanche when ascending Middagstinden. Two of the men managed to get out by themselves, but the two men at the back of the group died. On the 17th of March, 2013, another man was killed, but this time the location was Langfjellaksla, a mountain/mountain ridge on the south side of Kattfjordeidet.

An avalanche was released in Kroken Alpine Center on the 25th of Januray 2007, but luckily noone was killed. On February 26th, 2009, a girl lost her life after being swept away by an avalance on the north-west side of Nordfjellet, the mountain that Kroken Alpine Center is located on. On March 24th, 2013, a man was killed in an avalanche accident on the same side of Nordfjellet.

Sorbmegaisa was the scene of one of the worst avalanche accidents Norway has seen in the 20th and 21st century. Six ski tourists were buried by an avalanche which was classified as a very large avalanche on March 19th 2012. One person survived, but five of the skiers were killed. See Figure 5.1 for a map of the test site with the avalanche areas highlighted. More information about these accidents can be found at www.ngi.no.

5.3 Input data

Data files used in the classification of wet snow consists of SAR-images from 2005 to 2013 from the Envisat ASAR and the Radarsat-2 satellites, mask files containing information about lay-over and foreshortening, temperature information from the area, and a vegetation mask to filter out ocean, lakes, glaciers, and marshes.

The Radarsat-2 data has been geocoded based on either RS-2 SCNA Level 1B product or RS-2 SCWA Level 1B product, and the Envisat-data has been geocoded based on WSM (Wide Swath Medium resolution), and put on a common grid. The Level 1B SAR images are delivered by Kongsberg Satellite Services (KSAT), and the geocoding is performed at Norut. The original image is geocoded to a flat surface, and to get a correct mapping of the image, a DEM is used. This geocoding process also calculates the pixels affected by radar shadow or lay-over. More information about the geocoding process can be found in Lauknes and Malnes (2004).

The SAR data consists of 1668 images taken at different times and taken in different tracks, where the track number represents the satellite's orbit. This means that images with the same track number have the same geometry, and can be compared against each other. Stem plots of the number of SAR images available for each year is shown in Figure 5.2.

The mask files contain information about radar shadow, foreshortening and lay-over, and are the same size as the SAR images and contain values $\neq 0$ where there is lay-over and foreshortening. The vegetation mask has the same size as the SAR images, and has a pixel value of 44 where there is ocean, 41 where there is lakes, 36 for marshes, 34 for glaciers, and 0 elsewhere. Ocean, lakes, and marshes are masked out since the surface roughness of these areas will differ from image to image, and hence could possibly be wrongly classified as wet snow. These areas are shown in Figure 5.3.

5.4 Overview of the Snow Covered Area Wet algorithm

The SAR images are sent from Norut, already processed and geocoded. The images are grouped in a matrix called ImageGroup according to track number because the images for each track number will have the same incidence angle. Tracks with two or less images are left out due to lack of data to make

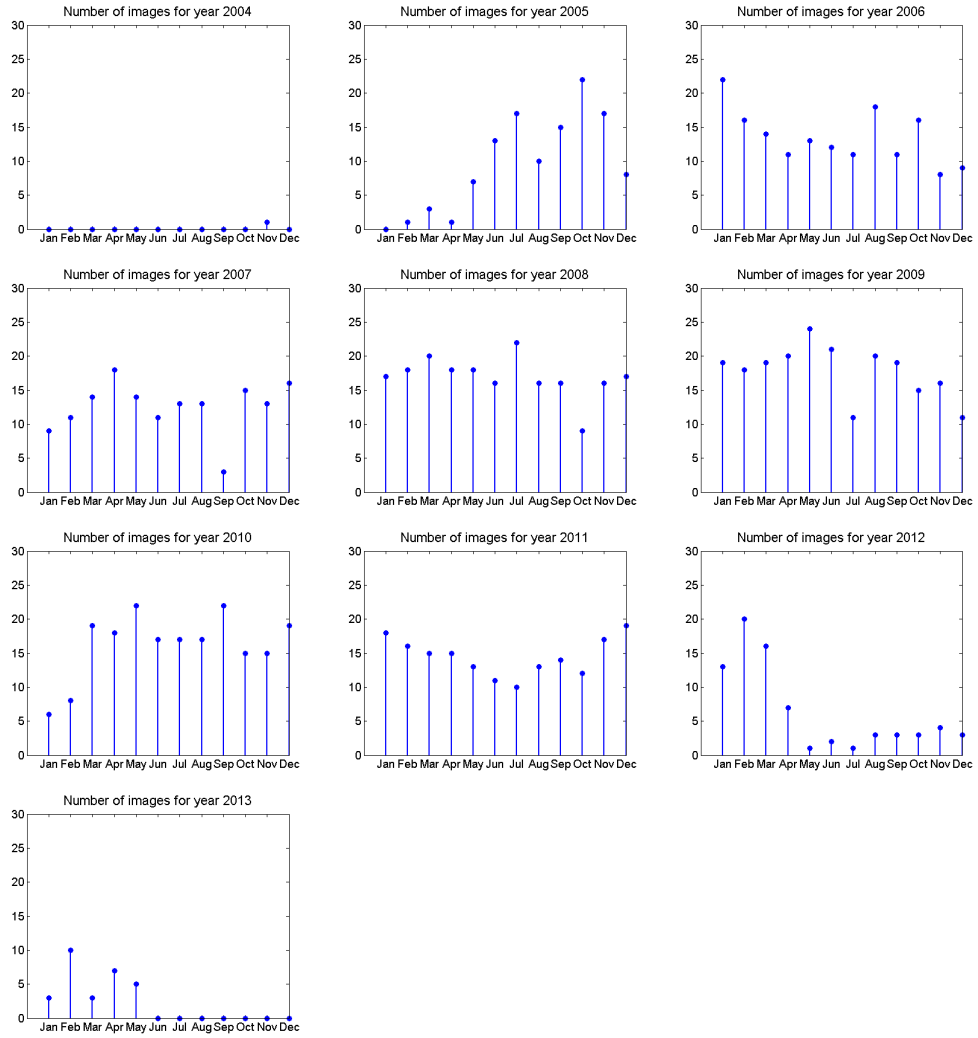

Figure 5.2: These stem plots show the number of SAR images available for every month in each year.

reference images. Originally there were 56 different tracks, but after excluding the tracks with less than three images, there were 48 tracks and 1658 images left. Date and time information for the different images are stored in the same matrix.

Reference images are made for each track group following three different methods, before one method is chosen to be the most suitable method. The SAR-images and the reference images are processed with the SCAW-algorithm. Figure 5.4 shows a simple diagram of the process. Afterwards, information about detected wet snow is used to make wet days-maps, were

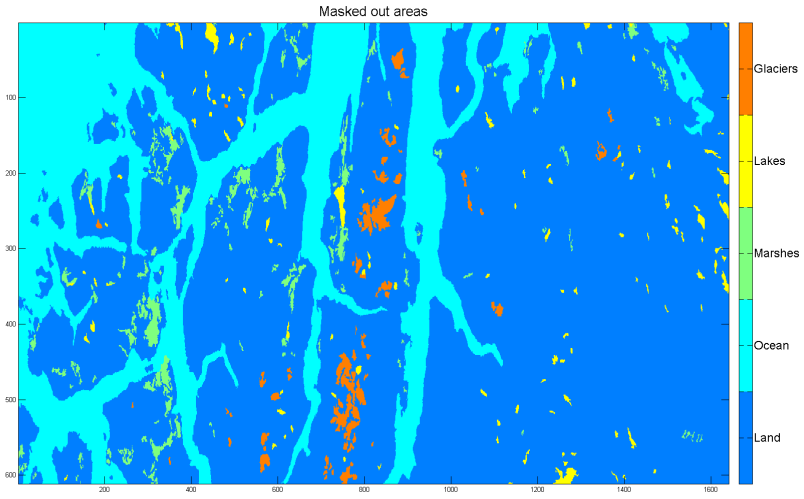

Figure 5.3: This is a color image of the vegetation mask where pixels of value 44 (ocean) are represented as light blue, pixels of value 41 (lakes) are represented by yellow areas, pixels of value 36 (marshes) are shown as green areas, and pixels of value 34 (glaciers) are shown as orange areas. Dark blue represents land pixels.

the wet snow pixels are summed up for each winter season, which is taken to last from the 1st of November to the 30th of April, to account for the total number of wet snow-days that season.

5.5 Reference images

Three different methods were used to find reference images, before one of the methods were chosen based on the detection results.

5.5.1 Reference method 1

This method uses one of the SAR images in each track as a reference image for that track. To find the most suitable SAR images, weather data from the five different weather stations mentioned in the test site section, is used. Weather data from the stations is loaded into matlab, and the dates of the SAR images are used to find the temperature at the different stations for those dates. It

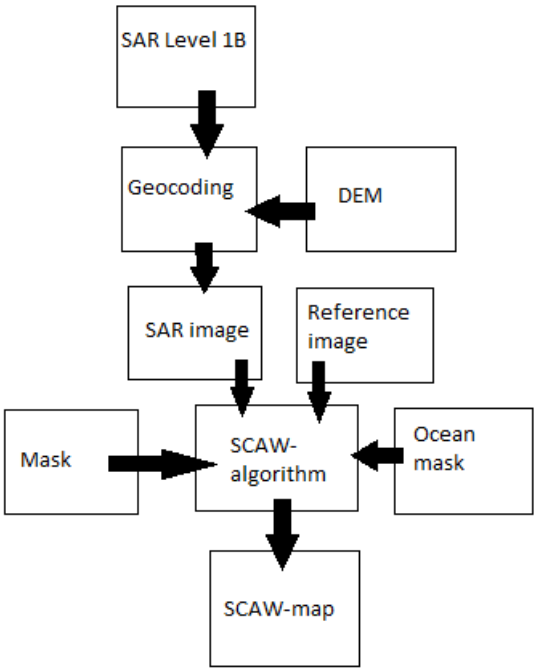

Figure 5.4: Block diagram of the process for wet snow detection

is desirable to find an image where there is only dry snow, so images from the five coldest days measured at the weather stations are compared. Since there are five stations, it is the five dates that occurred most frequent for all the stations that is chosen. Because the geometry of the images can differ so much (it might be that the coldest image, as one would consider to be the best image to be chosen as a reference image, could cover only the upper part of the test site, and therefore not be the most suitable reference image), a geometry threshold and a temperature threshold is used. The five images is compared against each other, and if the second coldest image has a better coverage than the coldest image, and the temperature of the second image does not exceed the temperature threshold, the second image will be chosen as a temporary best. This process is performed on all of the five images from all the tracks, and the image that has the best geometry while still being cold enough is chosen as a reference image for its track group.

The temperature threshold is set to be less than 0 degrees Celsius. The coverage is calculated by taking the amount of pixels with the value -50 or less (no coverage) and dividing it with the total amount of pixels in the image. Since there are five different temperatures for each image, a mean temperature is calculated by taking the mean of the five temperatures after all

the temperatures have been recalculated to represent sea level temperature. This is done by using the temperature correction shown in Equation5.1. If none of the images have a temperature less than 0 degrees, the reference image is set to be a matrix of NaNs (Not a Number), which means that there will not be a reference image for this track group, and thus, none of the images in the track group will be used in the SCAW-algorithm.

5.5.2 Reference method 2

This method uses the same five images as Method 1, but instead of choosing one of the images, all five are averaged to make a mean image. To correctly average the images, they first have to be converted to intensity images, instead of decibel images. The relationship between decibel and intensity is given as $I = 10 \cdot \log_{10}(dB)$. After the images are averaged into a reference image, the values are changed back into decibel values. This results in a reference image that is the mean of the images taken on the five coldest days. Because the images may have different coverage, it is important to only use pixels that actually have a real value. Thus, pixels with value -50 or less (no coverage) are discarded from the mean. If there aren't five images in one track group, the average is taken of the images available. Also, if the temperature for some of the images exceeds 0 degrees Celsius, they are discarded from the average.

The temperature for each image is calculated in the same way as the temperature in Method 1. If none of the images have a temperature less than 0 degrees, the reference image is set to be a matrix of NaNs (Not a Number), which means that there will not be a reference image for this track group, and thus, none of the images in the track group will be used in the SCAW-algorithm.

5.5.3 Reference method 3

In this method, all the images from September to April in one track group are averaged to make a mean reference image. To correctly average the images, they first have to be converted to intensity images, instead of decibel images. The relationship between decibel and intensity is given as $I = 10 \cdot \log_{10}(dB)$. After the images are averaged into a reference image, the values are changed back into decibel values. The time period is chosen to try to make sure that the images contain mostly dry snow or snowfree ground. To make sure

that the images do not contain too much wet snow, standard deviation is used to sort out images that, when taking the standard deviation, exceeds a certain threshold. This means that an average image has to be made from all the images available in the time period mentioned, before each image is subtracted from the mean.

The general definition of standard deviation is used, namely $\sigma = \sqrt{E(x-\mu)^2}$. As in Method 2, all pixels that have the value -50 or less (no coverage), are discarded from the calculations. If one or more images are discarded, a new mean image is made from the remaining images. The threshold for the standard deviation is set to 1.5 dB.

5.6 The Snow Covered Area Wet algorithm

When the preferable method for making reference images is found, the reference images can be used in the wet snow detection algorithm. This algorithm is based on the findings of Nagler and Rott (2000), which say that a signal drop of -3dB or more in snow covered areas when compared to a reference image, is likely to mean that the snow is wet.

To make the wet snow-maps, a matrix called SCAW (Snow Cover Area Wet), of the same size as the SAR images (611×1641), containing only zeroes, is created. A reference image and a SAR image from the same track group as the reference image are filtered by a 3×3-median filter to reduce speckle noise. Difference in backscatter is calculated by subtracting the reference image from the SAR-image. This difference image is called C. C is also filtered by a 3×3-median filter to reduce speckle noise even more. A difference of less than -3dB and bigger than -20 dB is chosen to classify wet snow, and pixels in the SCAW-matrix where ($C < -3$ & $C > -20$) are set to 0.8. The lower threshold of -20 dB is used to avoid classifying pixels that originally were pixels with no coverage (-50 dB or less) as pixels containing wet snow. The pixels with a C-value of less than -20 dB are set to 0.6, which is the value used for no coverage. Values between -3 dB and -2.5 dB are classified as possible wet snow, and pixels in the SCAW-matrix where ($-3 \leq C < -2.5$) are set to 0.95. To mask out areas that are without coverage, due to foreshortening and lay-over, the pixels in the SCAW-matrix are set to 0.6 where the pixels in the mask file accompanying the SAR image have values $\neq 0$. To mask out ocean and lakes, pixels in the SCAW-matrix are set to 0.4 where the pixels in the vegetation mask have the value 44 or 41. Glaciers and marshes can also contribute to false wet snow detection, so they are masked out by

setting SCAW to 0.2 where the pixels in the vegetation mask have the value 36 (marshes) or 34 (glaciers). Pixels in the SCAW-matrix containing dry snow (where the pixels in the difference image C have the value of 0 (pixels of no change)), are kept as zeroes. To stretch the colormap fully between 0 and 1, one pixel in the upper right corner is set to 1, and the neighboring pixel is set to 0.

The pixel values used in this algorithm are my own choices, and a table of the values can be found in Table 5.1. This algorithm is looped for each image in each track group. The resulting wet snow maps are compared to images from *www.senorge.no*.

Area	Threshold	Value
Wet snow	SCAW(C< -3 & C> -20)	0.8
Possible wet snow	SCAW($-3 \leq$ C < -2.5)	0.95
No coverage	SCAW(Mask $\neq 0$)	0.6
Ocean or lakes	SCAW(VegMask $= 44$ or $= 41$)	0.4
Marshes or glaciers	SCAW(VegMask $= 36$ or $= 34$)	0.2
Dry snow (no change)	SCAW(C $= 0$)	0

Table 5.1: An overview of the pixel values in the SCAW-matrices.

5.7 Detected wet snow fraction

To get a way of evaluating the three different reference methods, plots of the number of wet pixels divided by total amount of land pixels with coverage are made. The plots for each method are made by taking the SCAW images that are the result of the reference method and summing up the numbers of pixels that have the value of 0.8, which is the value of wet snow. The SAR images are divided into seasons, where each season consists of images from the 1st of November to the 31st of December for the first year, and images from 1st of January to the 30th of April from the following year. The total amount of land pixels with coverage are defined as pixels in the SCAW images that does not equal 0.4, 0.6 or 0.2, which means that ocean pixels, lakes, marshes, glaciers, and pixels with no coverage are excluded. This process is performed on all the SCAW images that results from the three reference methods. The 2004/2005 season is left out due to the fact that there are no SAR images from December 2004 or January 2005, and only one image for November 2004, as shown in Figure 5.2.

To make the plots easier to compare against the temperature derived wet snow fraction plots, each day that there is no SCAW data available the detected wet snow fraction values are linearly interpolated so we get a continuous curve. When there are two images for the same date, resulting in to wet snow fraction values for that date, the average wet snow fraction is found, and the two values are merged into one. The original wet snow fraction values, the pre-interpolation values, are plotted as blue circles in the same plot as the interpolated curve.

Snow height measurements from weather stations located in the test site are plotted together with the detected wet snow fraction.

5.8 Temperature derived wet snow fraction

To get some comparison data to the detected wet snow fraction plots, plots of land pixels with temperature above 1°C divided by the total amount of land pixels in the vegetation mask are made. The temperatures of the land pixels are calculated by taking weather data from Tromsø weather station (station number 90451), approximating it to sea level temperature by adding 0.006 times the elevation of the weather station to the temperature measured at the station, and then using a Digital Elevation Model (DEM) file, which contains the height above sea level for each pixel in the test area, and subtracting 0.006 times the pixel elevations from the temperature at sea level, as shown in Equation 5.1-5.3:

$$\begin{aligned} \text{Temp}_0 &= \text{Temp}_{st} + 0.006 * h && (5.1) \\ \text{TempMap}(i,j) &= \text{Temp}_0 - \text{DEM}(i,j) * 0.006 && (5.2) \\ \text{WetPixels} &= \sum_{i,j} (\text{TempMap}(i,j) > 1) && (5.3) \end{aligned}$$

where h is the height above sea level for Tromsø weather station, T_{st} is the temperature measured at the weather station, T_0 is the temperature at sea level, TempMap is a map of approximated temperatures for the whole test site, and WetPixels are the number of pixels in the temperature map with a value above 1°C. The sum of wet pixels is then divided by the number of land pixels that is not masked out by the vegetation mask. This fraction is calculated for each day in the the season time period mentioned earlier in this section. Land pixels in the vegetation mask are defined as pixels who do not have the value 44, 41, 36 or 34, thus excluding ocean, lake, glacier and marsh pixels.

The temperature maps shown in Figure 5.5 illustrates how the temperature derived wet snow fraction is found. The left side images are the temperature maps given as a result from Equation 5.2, while the images to the right are the results after Equation 5.3 is used, in addition to removing ocean, lake, glacier, and marsh pixels with the vegetation mask.

5.9 Scatter plots

Correlation between the detected wet snow fraction and the temperature derived wet snow fraction are plotted with the detected wet snow fraction data against the temperature derived wet snow fraction data, and marked by blue circles. Values of 0 and -1 are removed to make the plots easier to interpret. An ideal correlation line is plotted on top of the scatter plot, marked as a red line. A least squares regression line is plotted in grey. One correlation plot is made for every winter season and for each of the three reference methods.

5.10 Method for relating wet snow maps with avalanche activity

The test site is divided into four subareas, and wet snow maps are produced for these areas. This is done to study, in detail, the wet snow maps before the avalanche events. Three avalanche sections are made, even though there are four avalanche areas, because the two avalanche sites on Kvaløya, Langfjellaksla and Middagstinden, are situated close together. A fourth section is also made, see Figure 5.6, removing the inner mainland and the Lyngen peninsula, and keeping the island and the coastal part of the Tromsø mainland.

When making temperature derived wet snow fraction plots for the avalanche sections and the coastal region, the temperature maps are cropped so they cover the same area as the avalanche sites and the coastal part. When the snow depth data is collected, the weather station closest to the avalanche site is chosen, which means that Tromsø weather station is used for avalanche sites 1, 2, and 3, and Sørkjosen Lufthavn (station number 91740) is used for avalanche site 4, with the exception of season 2005/2006 and 2006/2007,

where Tromsø weather station is used due to the lack of snow data at station 91470.

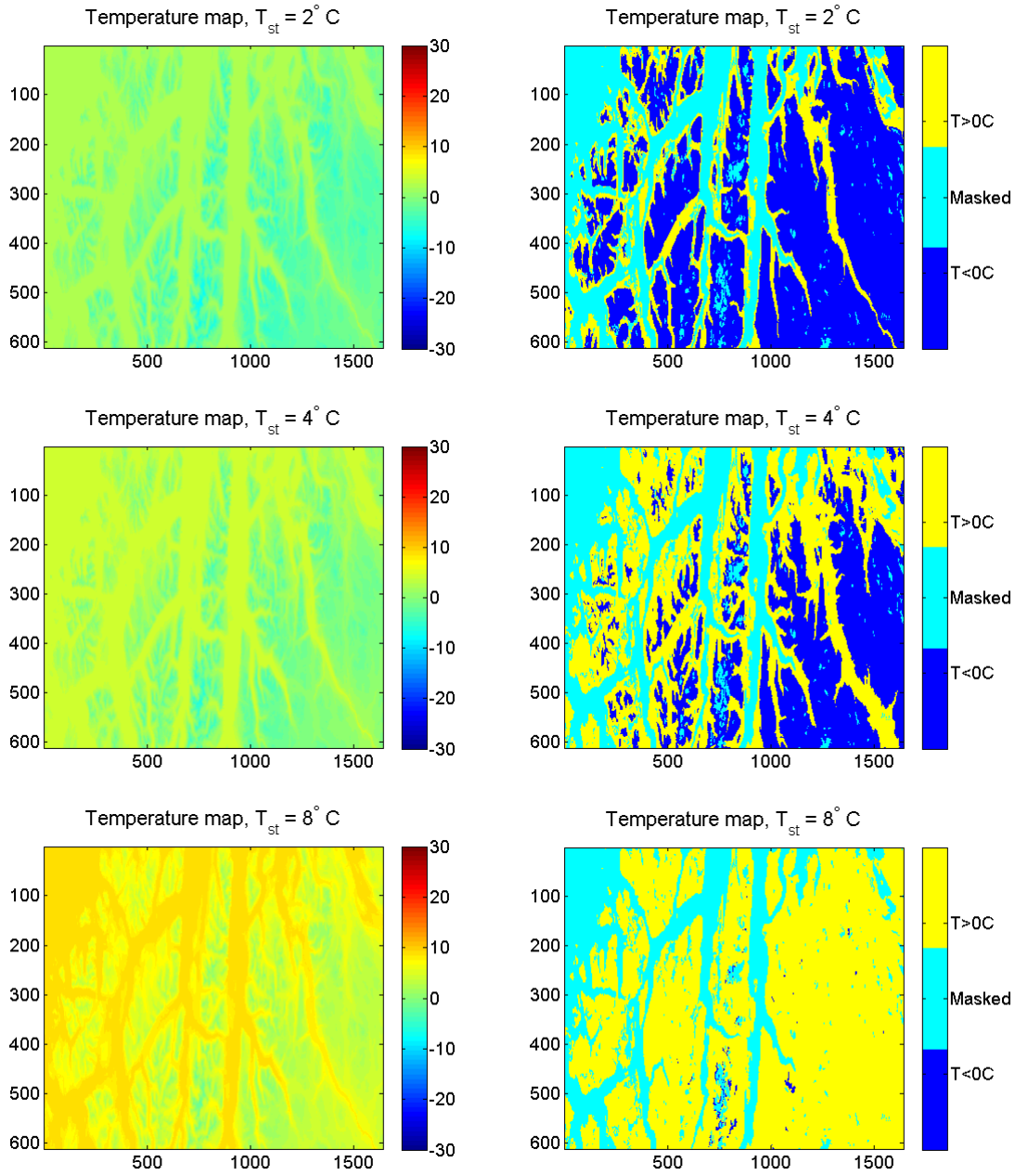

Figure 5.5: Left: Temperature maps of the test site for three different temperatures. The top image shows how the temperature map looks when the temperature in Tromsø is 2°C. The middel image shows the temperature map when the temperatur is 4°C. The bottom image show the temperature map when the temperature in Tromsø is 8°C. Right: The same temperature maps as on the left side, but the pixels with a temperature above 1°C are set to one value, the pixels with a value less than or equal to 1°C are set to another value, and areas masked out by the vegetation mask are given a third value.

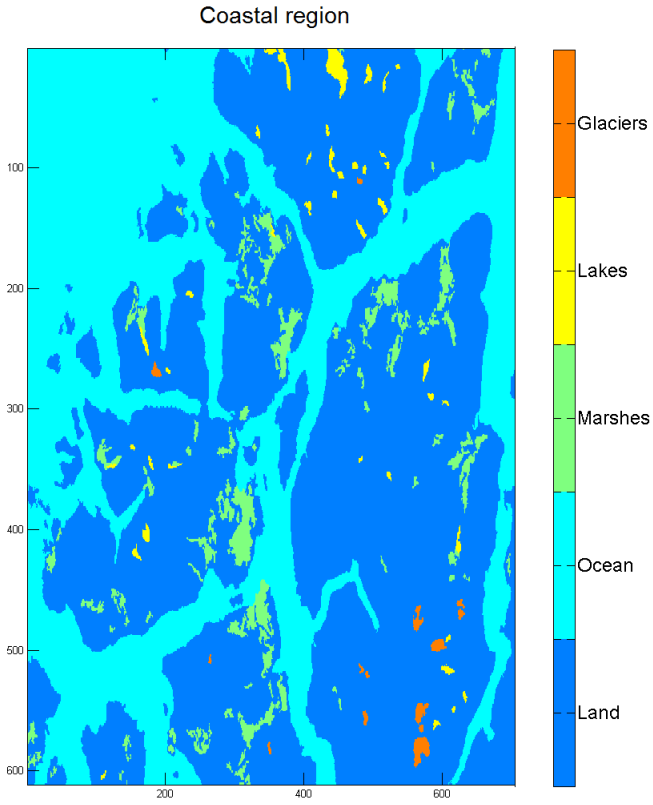

Figure 5.6: The coastal region of the test site, shown here with glaciers shown as orange areas, marshes shown as green areas, lakes marked with yellow areas, ocean shownas light blue areas, and bare ground marked with dark blue ares.

Chapter 6

Results

6.1 Wet snow maps

In this section we first study wet snow maps from each of the three reference methods developed in chapter 5, section 5.5.

Figure 6.1 shows a timeserie of SCAW maps for the 2006/2007 winter season made from reference method 1. Yellow indicates areas with wet snow, orange indicates areas with possible wet snow, green marks areas with no coverage, due to, e.g., foreshortening, lay-over, or bad geometry of SAR image, light blue marks oceans and lakes, blue marks glaciers and marshes, and dark blue indicates areas covered with dry snow or bare-ground. In Figure 6.1 we observe that there was mostly dry snow or no snow from November to March 12th. On March 12th we see large areas covered in wet snow and possible wet snow. These areas are gone on March 13th and March 20th, for so to reappear on March 26th, and gradually increase in size as spring melt sets in.

Figure 6.2 shows a timeserie of SCAW maps, also for the 2006/2007 winter season made from reference method 2. The timeserie shows mostly dry snow or bare ground from November to March 26th. There are signs of wet snow on March 12th, but not nearly in the same amount as in Figure 6.1.

Figure 6.3 shows a timeserie of SCAW maps for the same season made from reference method 3. It is very similar to the figure made from method 2, and does not show any snowmelt of particular importance until March 26th.

We observe that the main detection of wet snow seems to happen in areas

of higher elevation, and that there are low amounts of detected wet snow in the lowlands. The SCAW maps made with reference method 1 seem to have the highest detection of wet snow, the SCAW maps from method 3 seem to have the second highest, and the SCAW maps from reference method 2 seem to have the lowest detection, even though the five last maps in the three figures appear to have almost the same amount of detected wet snow. One interesting observation is that on April 29th, the last image in the timeseries, the wet snow map from method 3 seems to the highest detection of wet snow, with method 2 having the second highest, and method 1 having the lowest detection. These findings are studied in more detail in section 6.3.

6.2 Standard deviation of backscatter in reference method 2 and 3

The standard deviation of the radar backscatter for the different reference methods may provide insight into the accuracy of the various methods. It is a measure of how much the backscatter in images that make up the averaged reference images differ from the backscatter in the same reference images. Since reference method 1 only uses one scene, this method cannot be judged in the same way, but for reference method 2 and 3 we have calculated the pixel vise standard deviation for each track.

Figure 6.4 shows a plot of the standard deviation of backscatter in the reference images used in method 2, and the standard deviation of backscatter in the reference images used in method 3 before and after removal of outliers. We notice from Figure 6.4 that method 2 on average has lower standard deviation than method 3, but after removing the outliers the standard deviation of method 3 is reduced.

Standard deviation values of 0 means that the reference image consists of only one image. The lack of a standard deviation value for a track means that the track did not have suitable images available to make a reference image.

6.3 Wet snow fraction plots

The percentage of wet snow pixels found in SCAW maps compared to total amount of land pixels in the same map, is called detected wet snow fraction.

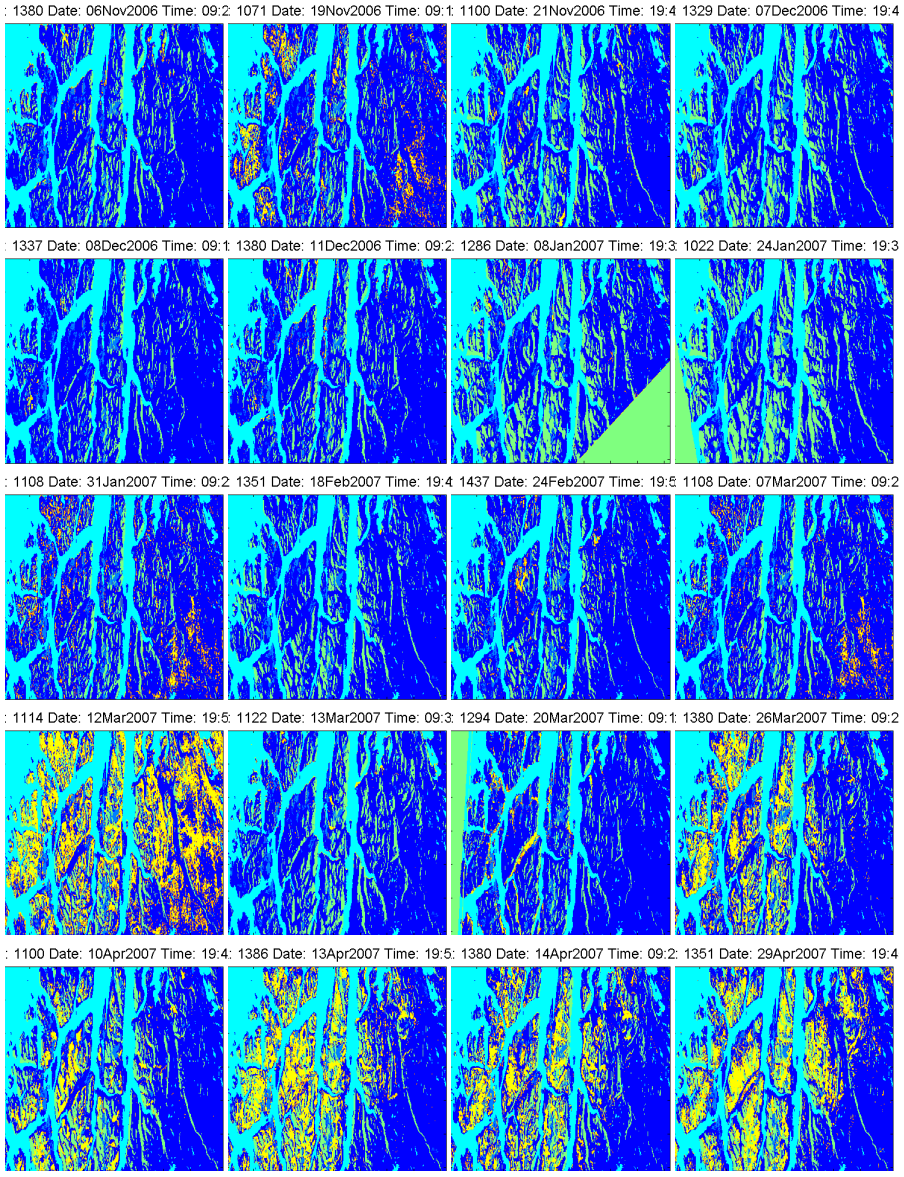

Figure 6.1: A timeserie of SCAW maps made with reference method 1.

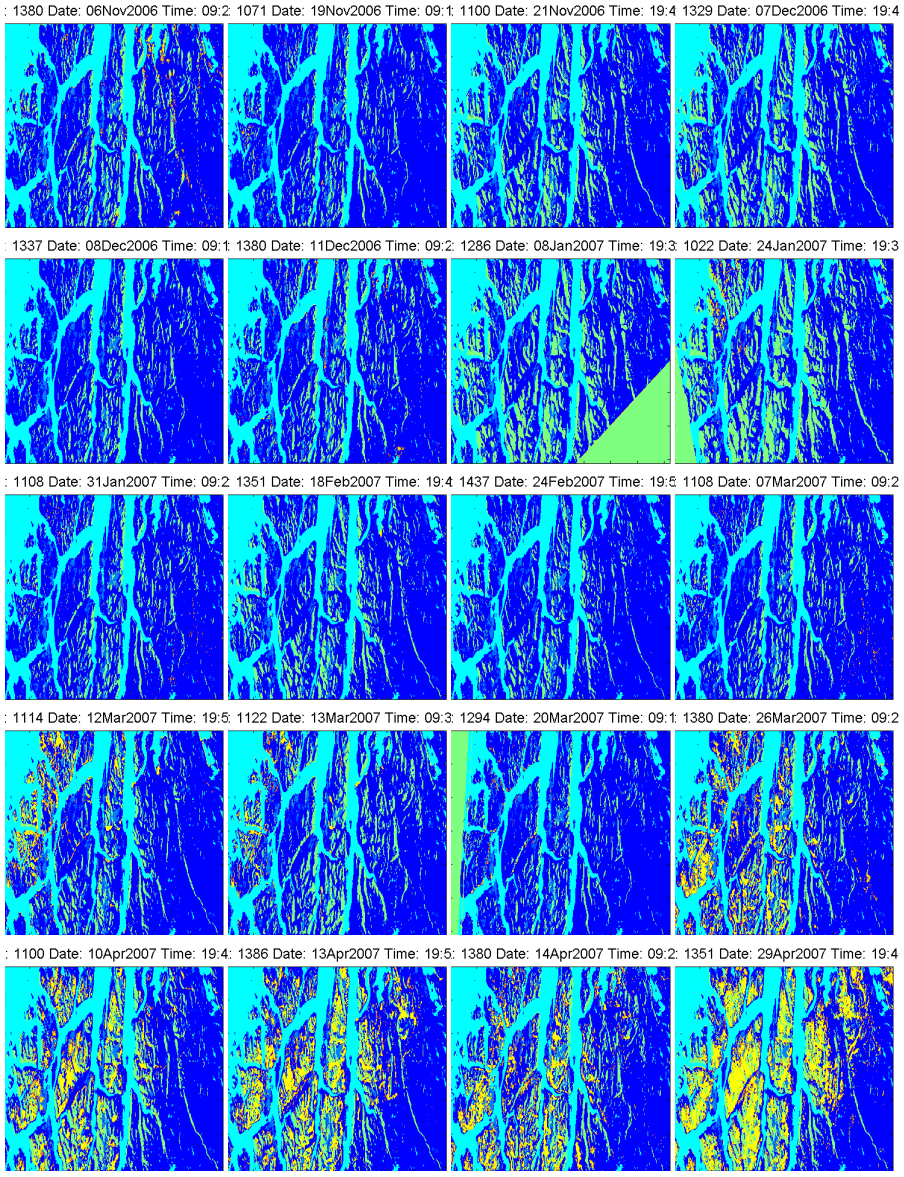

Figure 6.2: A timeserie of SCAW maps made with reference method 2.

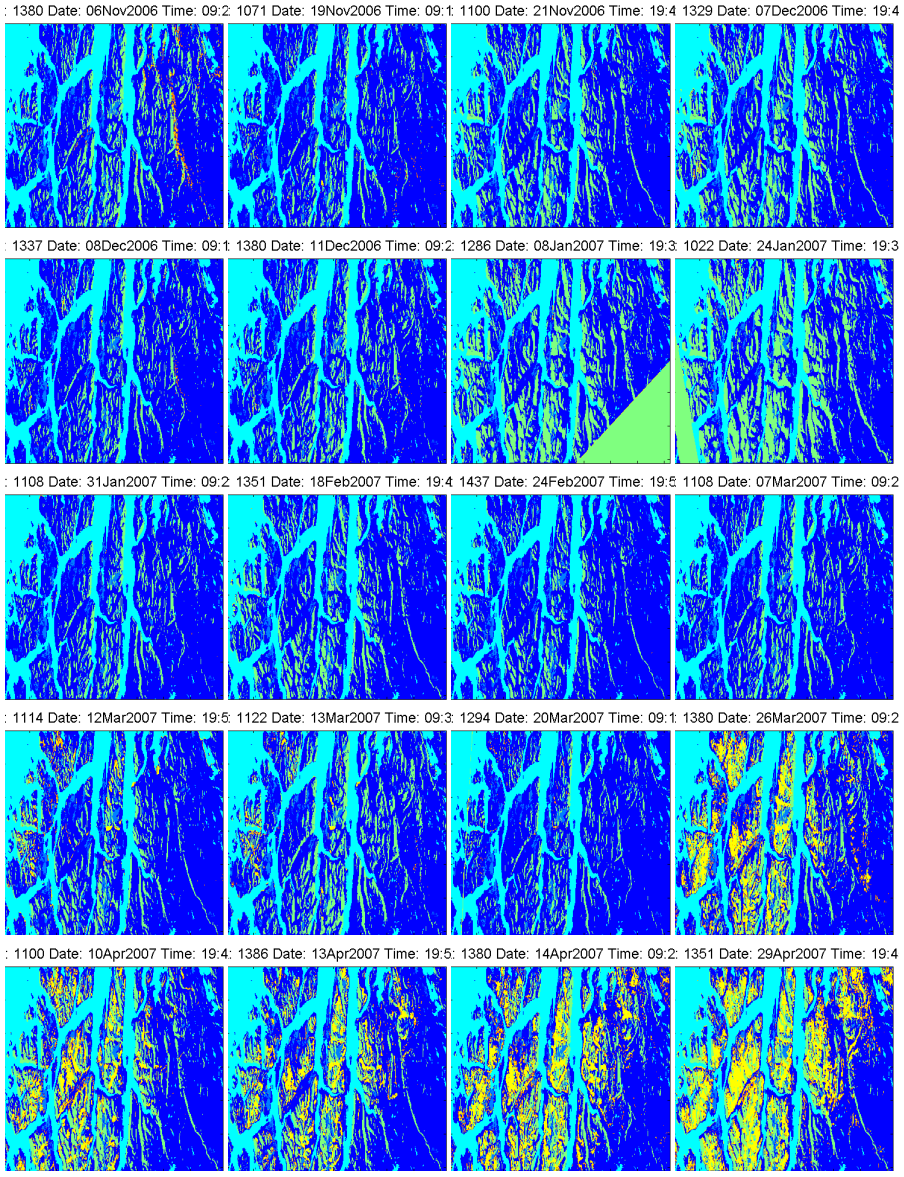

Figure 6.3: A timeserie of SCAW maps made with reference method 3.

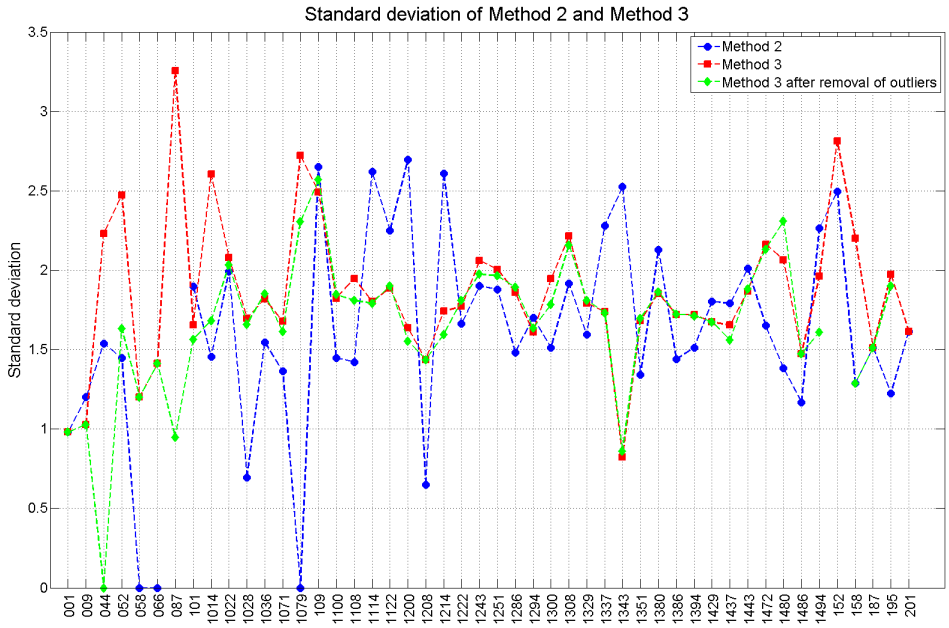

Figure 6.4: A plot of the standard devation for backscatter in reference images from method 2 and 3 for the different tracks. The blue line represents method 2, the red line represents method 3 before removal of outliers, and thre green line represents method 3 after removal of outliers.

The percentage of pixels with a temperature above 1°C found in temperature maps made according to equations 5.1-5.3, compared to total amount of land pixels, is called temperature derived wet snow fraction. Land pixels are defined as the pixels in the vegetation mask that are not glacier, marsh, lake, or ocean pixels.

6.3.1 Reference method 1

Two wet snow fraction plots from method 1 are shown in the top part of figures 6.5 and 6.6. In the top plot in Figure 6.5 we observe detected wet snow in the end of December, and a decline in snow depth in the same time period. The top plot in Figure 6.6 shows small amounts of detected wet snow until early April. In April, when the springmelt sets in, we expect to find large amounts of wet snow. This is seen in the detected wet snow fraction plot, and as a steady decline in the snow depth. In both plots the detected wet snow fractions are lower than the temperature derived wet snow fractions, which are seen in the bottom plots of the two figures. We also see that there are times when the temperature derived wet snow fraction plots indicate that there is no wet snow, but the detected wet snow fraction plots indicate that there is wet snow. An example of this is found around April 17th 2011, where the detected wet snow fraction values go from 30% to 40% and the snow depth goes from 60 cm to nearly 80 cm. In both figures we observe that method 1 has the highest values of detected wet snow.

6.3.2 Reference method 2

The two detected wet snow fraction plots from method 2 are shown second from the top in figures 6.5 and 6.6. The plot in Figure 6.5 shows signs of snow melt around December 20th, but the amounts of detected wet snow are smaller that that of the method 1 plot at the top of the same figure. There is an overall tendency for the detected wet snow fraction values of method 2 to be lower than those of method 1. The same tendency is seen in Figure 6.5 as well, but there is a significantly higher value of detected wet snow just before April 5th in the method 2 plot, seen when compared to the method 1 plot.

6.3.3 Reference method 3

The detected wet snow fraction curves from method 3 are shown in the second to last plots in figures 6.5 and 6.6. The plot in Figure 6.5 bear a resemblance to the plot from method 1 in the same figure, only with lower values. The biggest differences are found just after December 20th, March 11th, March 13th, and just before April 17th. On these dates, the method 3 values are a lot lower than those of method 1. Compared to the plot of method 2, the method 3 values are higher on most dates, except for March 17th, where the method 2 wet snow values are higher. In Figure 6.6 the method 3 looks more similar to the curve of method 2 than that of method 1. There is only a slight difference in the wet snow values before March 5th, April 5th and after April 17th. On those dates, the method 2 values are higher than the method 3 values.

Temperature derived wet snow

The bottom parts of the figures are temperature dependent wet snow fraction plots. The temperature derived plot of Figure 6.5 shows large amounts of wet snow in the last half of November and the first weeks in December. This does not show up in the detected wet snow plots in the same figure. The snow depth curve shows the presence of snow, at least in Tromsø city, and that the snow depth is declining in this time period. The temperature derived wet snow fraction plot in Figure 6.6 and the detected wet snow fraction plots in the same figure all show the same pattern, only that the detected wet snow values are lower than the temperature derived values, especially early in the winter season, when there is little or no snow present.

The scale on the y-axis differs from the bottom and the above plots, with a scale of 0-100% for the detected wet snow fraction plots and a scale of 0-200% for the temperature derived wet snow fraction plots. This is done to make the plots easier to read. Values of -1 in the detected wet snow fraction plots are used when there is no SAR data available.

6.3.4 Wet snow in the coastal region

In this section we check if the correlation is better in the coastal region between the detected wet snow fraction and the temperature derived wet snow fraction, as the weather station used to derive the temperature derived

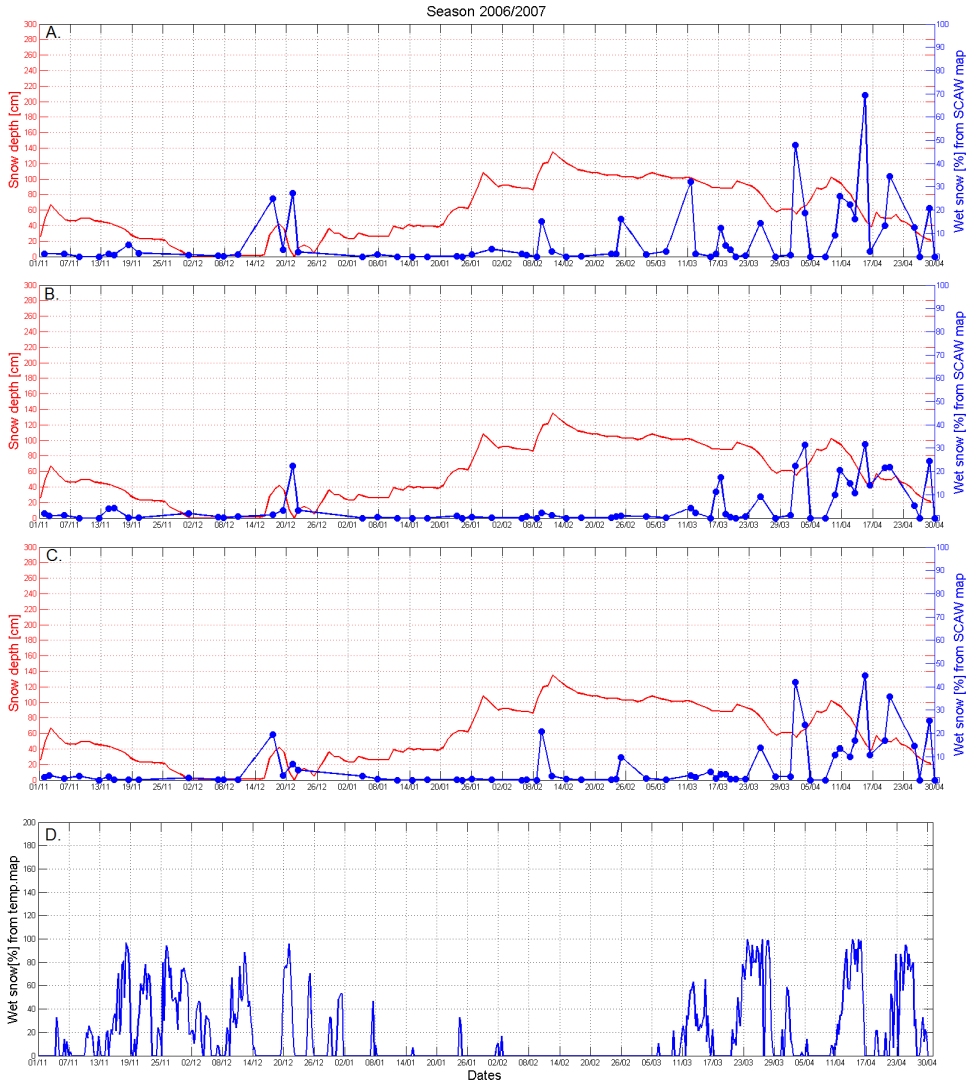

Figure 6.5: A: Detected wet snow fraction plot created with reference method 1. B: Detected wet snow fraction plot created with reference method 2. C: Detected wet snow fraction plot created with method 3. D: Plot of temperature derived wet snow fractions. All plots are from the 2006/2007 winter season. The blue dots mark the real values for the SCAW wet snow fraction. The blue line shows the interpolated values of the wet snow fraction, and the red line shows snow depth.

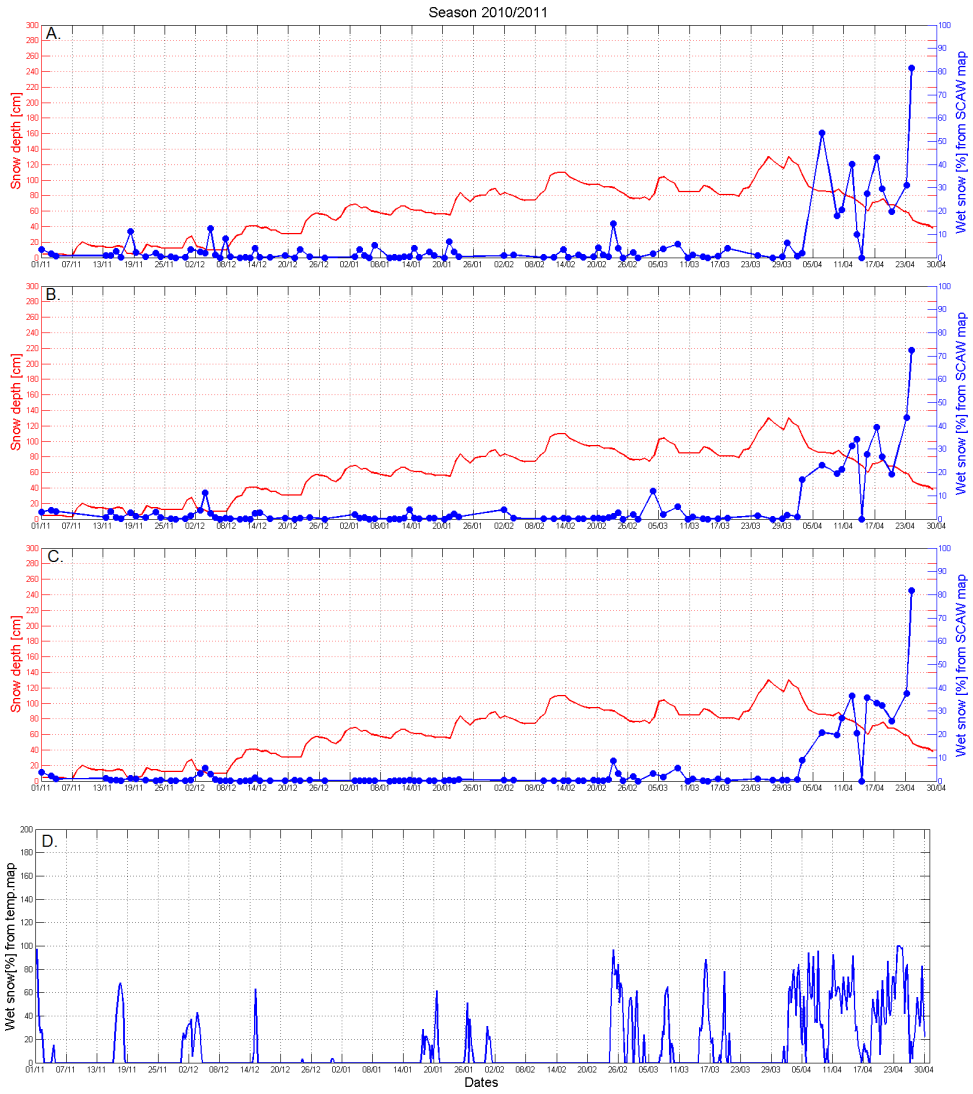

Figure 6.6: A: Detected wet snow fraction plot created with reference method 1. B: Detected wet snow fraction plot created with reference method 2. C: Detected wet snow fraction plot created with method 3. D: Plot of temperature derived wet snow fractions. All plots are from the 2010/2011 winter season. The blue dots mark the real values for the SCAW wet snow fraction. The blue line shows the interpolated values of the wet snow fraction, and the red line shows snow depth.

wet snow fraction is situated in Tromsø city. Tromsø is located close to the coast, and here we only study the western part of the test site. See Figure 5.6 for an illustration of the area in question. Wet snow fraction plots from the coastal region for the 2006/2007 winter season and the 2010/2011 winter season are seen in figures 6.7 and 6.8.

Reference method 1

The detected wet snow fraction plots of method 1 is shown in the top part of Figures 6.7 and 6.8. When comparing the method 1 plot in Figure 6.7 too the one in Figure 6.5 we observe that several peaks in the curve have disappeared or been greatly reduced. This can be seen around December 14th, February 8th, February 26th, and around April 23rd. The remaining peaks in the coastal wet snow curve have increased slightly. Looking at the plot from method 1 in Figure 6.8 we see a large increase in the peak at November 19th compared to the plot of the whole test site. All the other detected wet snow values have also increased, except for one value between April 11th and April 17th. Here the detected wet snow fraction value has gone down from 20% to 0%.

Reference method 2

Two detected wet snow curves of method 2 are shown in the plots second from the top in Figures 6.7 and 6.8. In Figure 6.7 we see an increase in the values of detected wet snow compared to the method 2 values in Figure 6.5. The only decrease in detected wet snow values from Figure 6.5 to Figure 6.7 is found around April 17th 2007, where the wet snow value to the left of this date has gone from over 30% wet snow to 0%, and between April 17th and April 23rd, where one of the values has gone from 20% to 0% wet snow. Studying the method 2 plot in Figure 6.8 and Figure 6.6, it becomes apparent that there is a general increase in almost all of the detected wet snow fraction values, except for one value between April 11th and April 17th, where the value has gone from over 30% to 0% detected wet snow.

Reference method 3

Detected wet snow fraction curves from method 3 is shown in the second to last plots in Figures 6.7 and 6.8. When comparing the plot in Figure 6.7 and Figure 6.5, we observe that the peak between December 14th and December

20th has disappeared. So have the peak just after February 8th and the one before February 26th. The value to the left of April 5th and the value to the left of April 17th have been reduced. The rest of the detected wet snow fraction values in the method 3 plot in Figure 6.7 have increased. In the plot in Figure 6.8, we see an overall increase in the amount of detected wet snow, compared to the plot in Figure 6.6. Also here, as in the two plots from the other reference methods in Figure 6.8, has the amount of wet snow between April 11th and April 17th decreased.

Temperature derived wet snow

The temperature derived wet snow fraction plots are shown in the bottom part of Figures 6.7 and 6.8. These plots are almost identical to the temperature derived plots in Figures 6.5 and 6.6, except for a slight increase in all the wet snow fraction values in the temperature derived plots for the coastal region.

The temperature maps that the temperature derived wet snow fraction plots are based on, are cut to fit the area of the coastal region.

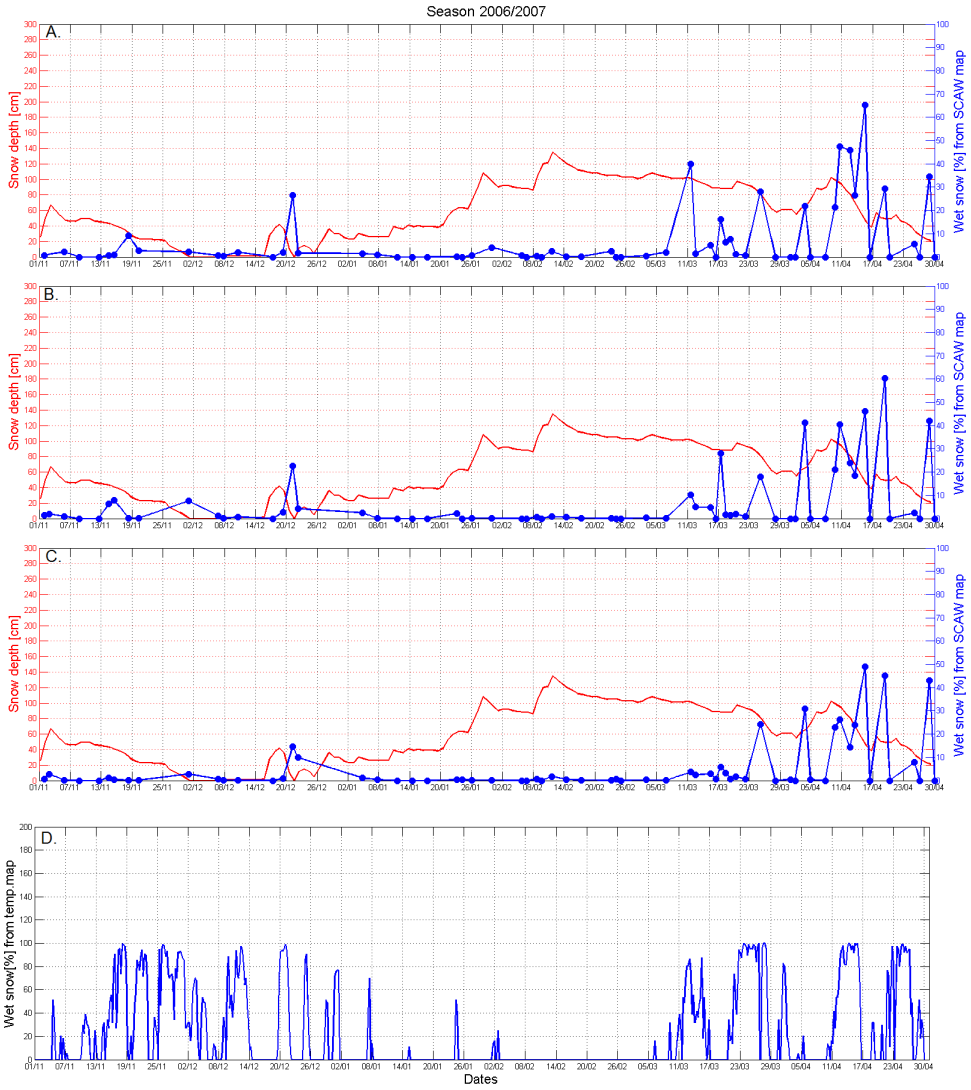

Figure 6.7: A: Detected wet snow fraction plot for the coastal region. Method 1 is used. B: Detected wet snow fraction plot for the coastal region. Method 2 is used. C: Detected wet snow fraction plot for the coastal region. Method 3 is used. D: Plot of temperature derived wet snow fractions. All plots are from the 2006/2007 winter season. The blue dots mark the real values for the SCAW wet snow fraction. The blue line shows the interpolated values of the wet snow fraction, and the red line shows snow depth.

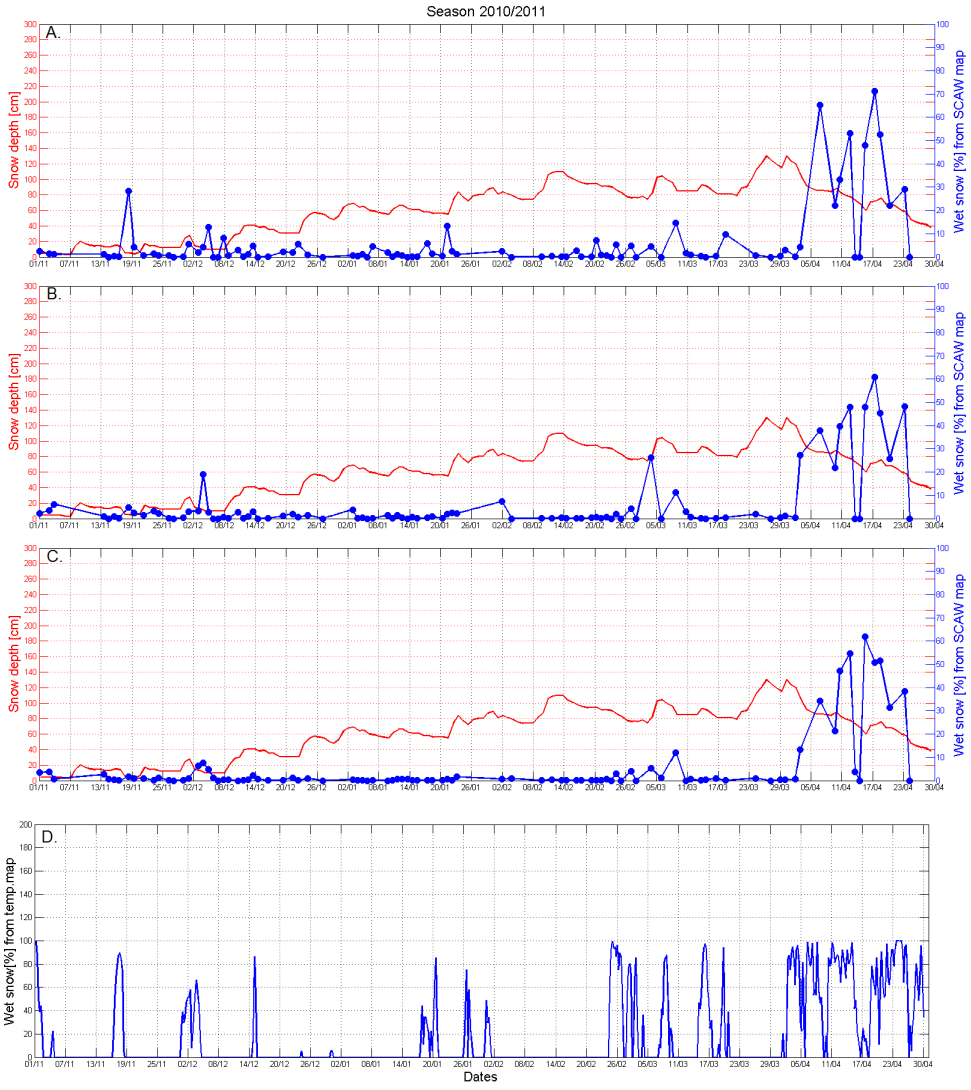

Figure 6.8: A: Detected wet snow fraction plot for the coastal region. Method 1 is used. B: Detected wet snow fraction plot for the coastal region. Method 2 is used. C: Detected wet snow fraction plot for the coastal region. Method 3 is used. D: Plot of temperature derived wet snow fractions. All plots are from the 2010/2011 winter season. The blue dots mark the real values for the SCAW wet snow fraction. The blue line shows the interpolated values of the wet snow fraction, and the red line shows snow depth.

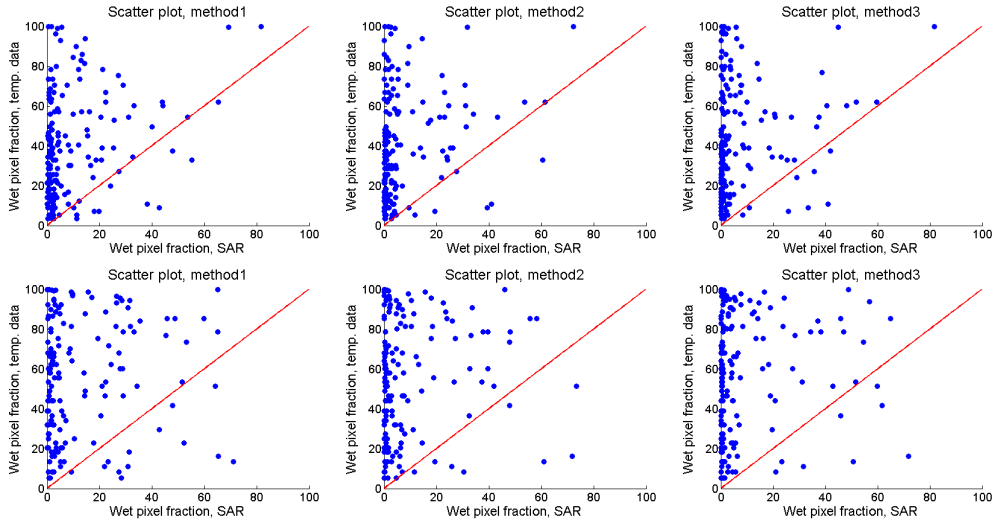

Figure 6.9: Top: Scatter plots of detected wet snow fraction and temperature derived wet snow fraction for the three reference methods. Bottom: Scatter plots of detected wet snow fraction and temperature derived wet snow fraction for the coastal region. The red line represents ideal correlation.

6.4 Correlation between detected and temperature derived wet snow fraction

The detected wet snow fraction data from the previous section is plotted against the temperature derived wet snow fraction data in a scatter plot. This is done to show the correlation between the two data sets. Fraction values of 0 are removed to make the plots more readable. The values of -1, which represent the value of the detected wet snow fraction when there is not any detected wet snow fraction data available, are also removed. The red line represents ideal correlation (1:1).

The detected wet snow fraction data and the temperature wet snow fraction data is gathered for all the season for each reference method and plotted. This means that there is one scatter plot for each reference method, shown in the top part of Figure 6.9. We observe that most of the data points lie close to the y-axis for the three plots. There are few points along the ideal correlation line. In the bottom part of Figure 6.9, the correlation plots for the coastal section of the test site are shown. We see that the correlation is somewhat better, but also here, many data points lie along the y-axis, or close to it, and few points lie along the red line.

6.5 Relation between wet snow and avalanches

The SCAW maps are divided into smaller sections that emphasized the avalanche accidents areas. The avalanche sites on Middagstinden and Langfjellaksla are chosen as avalanche section 1 and 2. They are merged into one section, since they are close in distance (both sites are located in Kattfjordeidet, Kvaløya). Kroken is chosen as avalanche section 3, and Sorbmegaisa is chosen as avalanche section 4.

6.5.1 Avalanche site 1 and 2

A timeserie of SCAW maps for the 2005/2006 winter season up to the avalanche accident on February 19th 2006, where a skier was taken by an avalanche on Middagstinden, is shown in Figure 6.10. Looking at the wet snow fraction plot for the 2005/2006 winter season in Figure 6.11, we see high values of detected wet snow in the first half of January and in the beginning of February. The snow depth goes from 30 cm to 0 cm in January. During the detected snowmelt in February, where there was a high amount of detected melting snow (around 50% wet snow), we see an increase in snow depth from 0cm to 20cm, and a small peak in the curve between February 8th and February 14th. Right before the avalanche event of February 19th, we observe a peak in the detected wet snow fraction curve, but no decrease in snow depth.

In the 2006/2007 season plot, we find snowmelt in November and around December 20th. Between those dates there few signs of the presence of wet snow, and after December 20th, there are no significant peaks in the wet snow curve until March 11th.

If we look at the wet snow fraction plot for the 2007/2008 winter season, we see a couple of peaks in the wet snow curve that indicates high amounts of wet snow in January and February. The snow depth curve shows that there was little to no snow during the first two months of the winter season.

Almost the same pattern as seen in the wet snow fraction plot for the 2005/2005 season can be found in the 2008/2009. The main differences are the snow depth, which is higher for the 2008/2009 season, the peak in the wet snow curve just before November 13th 2008, which is not found in the 2005/2006 plot, and that the amount of detected wet snow is higher in same season.

The 2009/2010 season, shown in Figure 6.12, reveal large amounts of detected wet snow early in the season, even though the snow depth curve indicates that there is no snow at that time (not for Tromsø city, at least). There are some periods of wet snow late in January and early in February, accompanied by a decrease in snow depth.

There are low amounts of detected wet snow before spring melt sets in in the plot of the 2010/2011 season, except around November 19th and January 20th, where we find two peaks in the detected wet snow curve.

In the wet snow fraction plot for the 2011/2012 winter season, there are indications of wet snow on November 13th and in the first half of January. I the beginning of February we have two large peaks in the wet snow curve before the avalanche accident at the 18th of February 2012. One peak between February 8th and February 15th that exceeds 40% wet snow cover, and one peak just after the 15th that reaches 30% wet snow cover.

The 2012/2013 season is harder to assess, due to the lack of SAR data for that season, but we can still see, cf. the high peak around February 23rd 2013 in Figure 6.12, that there was at least one SAR image which showed melting snow before the avalanche at March 17th 2013.

6.5.2 Avalanche site 3

The wet snow fraction plot from the 2005/2006 winter season in Figure 6.14 shows detected snowmelt in December and January, and there is a decrease in the snow depth during the first part of January. We also find peaks that indicate the presence of wet snow in the end of January and in the beginning of February. Then there are low amounts of detected wet snow until the end of April.

In the 2006/2007 plot there is nearly no detected snowmelt in the first four months of the season, except for one peak around December 20th 2006 that reaches almost 40% wet snow and coincides with a rapid decrease in snow depth. Between the peak and the avalanche event on January 25th, there are no signs of detected wet snow. The snow depth grows steadily from the end of December to after the avalanche is released.

The plot from the 2007/2008 winter season shows that there was a high amount of detected wet snow in January and February that season, with high peaks in the wet snow curve just before December 14th, on January

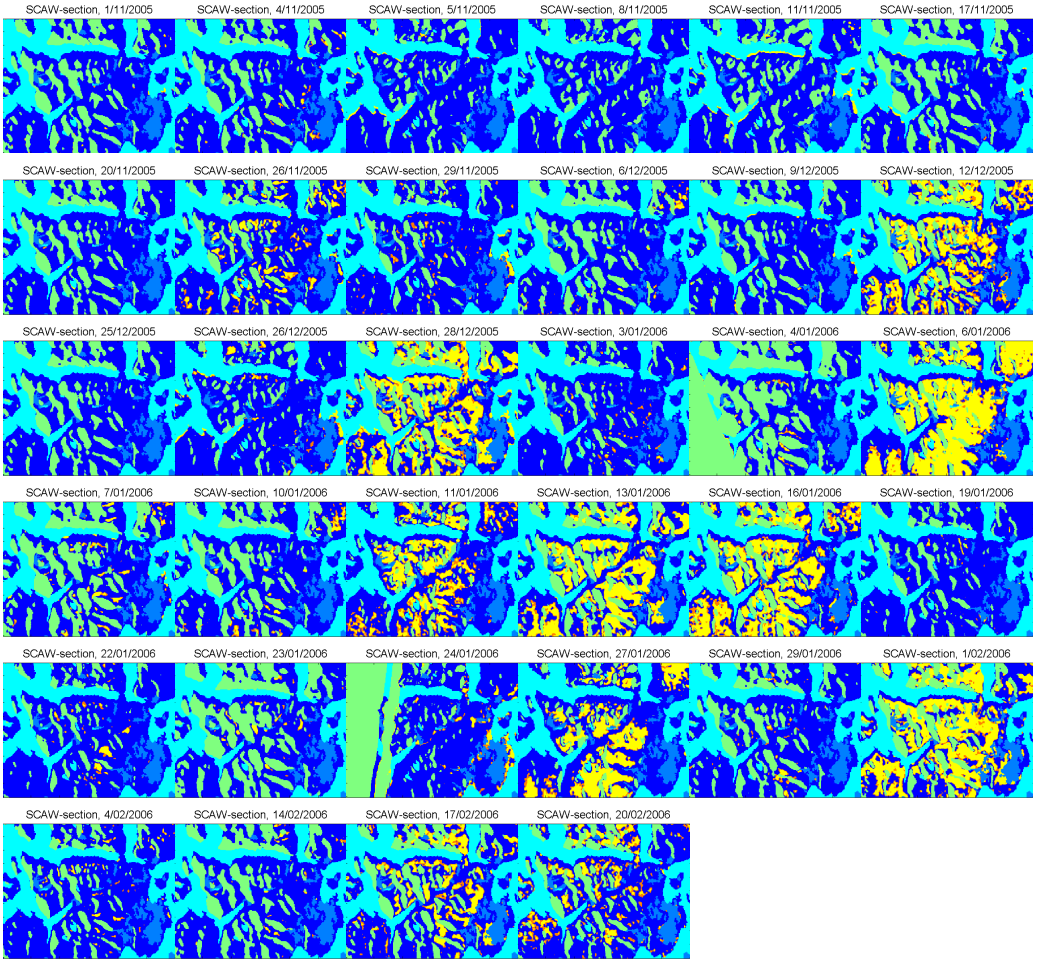

Figure 6.10: Timeserie of the 2005/2006 winter season from November 1st 2005 to February 20th 2006 for avalanche site 1 and 2. Yellom areas represent wet snow, orange areas represent possible wet snow, green areas are areas with no coverage, dark blue areas represent dry snow or land, blue areas are marshes, and light blue areas are ocean.

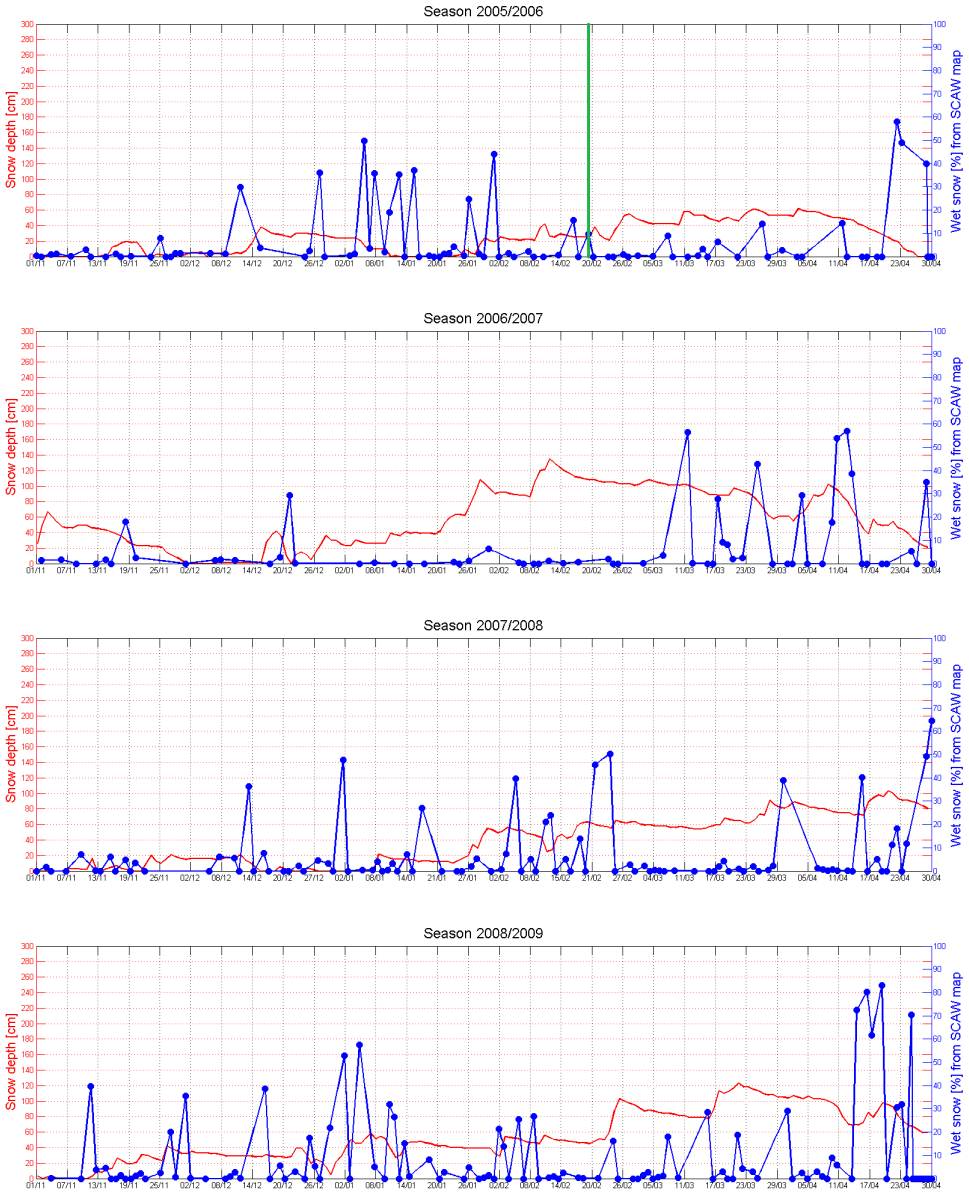

Figure 6.11: Detected wet snow fraction plot for avalanche site 1 and 2 for the winter seasons, starting with the 2005/2006 season in the top image, and ending with the 2008/2009 season in the bottom image. The green, vertical line in the top image marks the avalanche accident at Middagstinden, February 19th 2006. Method 1 is used as reference method. The blue dots mark the real values for the SCAW wet snow fraction. The blue line shows the interpolated values of the wet snow fraction, and the red line shows snow depth.

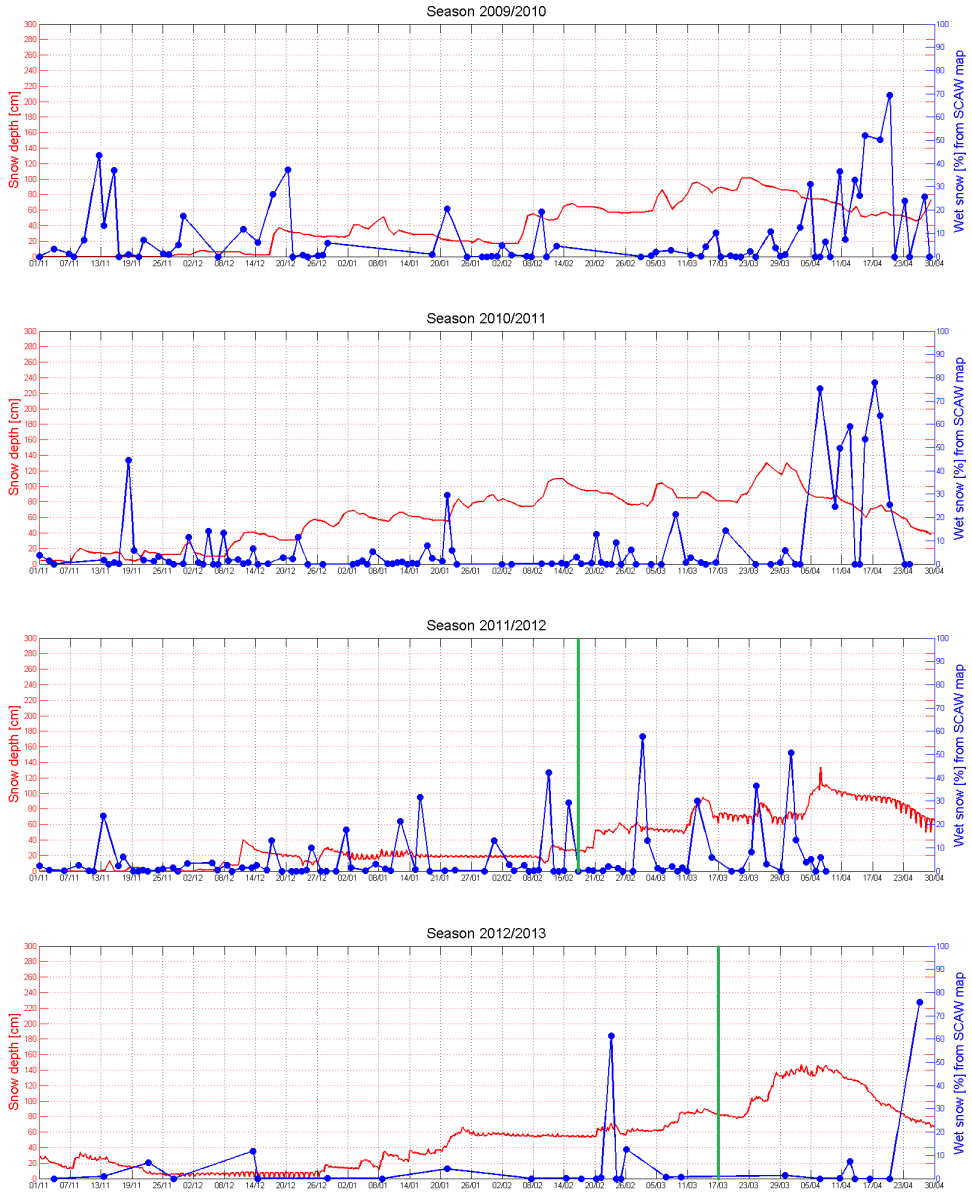

Figure 6.12: Detected wet snow fraction plot for avalanche site 1 and 2 for the winter seasons, starting with the 2009/2010 season in the top image, and ending with the 2012/2013 season in the bottom image. The green, vertical line in the second to last image marks the avalanche accident at Middagstinden, 18th February 2012. The green, vertical line in the last image marks the avalanche accident at Langfjellaksla, 17th March 2013. Method 1 is used as reference method. The blue dots mark the real values for the SCAW wet snow fraction. The blue line shows the interpolated values of the wet snow fraction, and the red line shows snow depth.

2nd, between January 14th and January 21st, and two twin peaks that both exceeds 50% wet snow in the end of February.

A timeserie of SCAW maps covering the area for the 2008/2009 winter season up to the day of the accident on February 26th 2009, is shown in Figure 6.13. In the wet snow fraction plot from the 2008/2009 season, we see indications of high amounts of melting snow in the first two and a half months of the season, reaching fraction values above 50% in the beginning of January. There is a dip in the snow depth curve between December 26th and January 2nd, and two smaller dips before January 14th and on February 2nd. In the time between January 14th and the avalanche accident on February 26th, the amount of detected wet snow is low. Right before the avalanche is released we see a rapid increase in the snow depth, going from just over 20cm to over 100cm of snow on only a few days.

The plot from the 2009/2010 season in Figure 6.15 shows that the highest values of detected wet snow were found in November and December 2009. There are some small peaks around the end of January and beginning of February, but nothing of apparent significance.

The next season shows almost no snowmelt until spring, only a small peak just before November 19th, while the 2011/2012 season has some sparsely placed peaks indicating snowmelt. We observe one peak on November 13th and two larger peaks, one between February 8th and February 15th, and one in the beginning of March. The snow depth is quite stable for the first three and a half months of the season.

In the 2012/2013 winter season there is a clear likeness to the 2012/2013 season for avalanche site 1 and 2, with one fairly high peak before the avalanche accident on March 24th 2013. This is probably due to a warm period in February that season.

6.5.3 Avalanche site 4

In the 2005/2006 plot in Figure 6.17 we observe some small peaks in the wet snow curve during the season, but nothing above 20% until April. In the 2006/2007 plot we find some higher peaks, particularly one between December 14th and December 20th, and in the end of February and the beginning of March. The 2007/2008 season show some small peaks in the wet snow curve that coincides nicely with the decreases in the snow depth. The wet snow plot from the 2008/2009 season has some peaks in the first half of January.

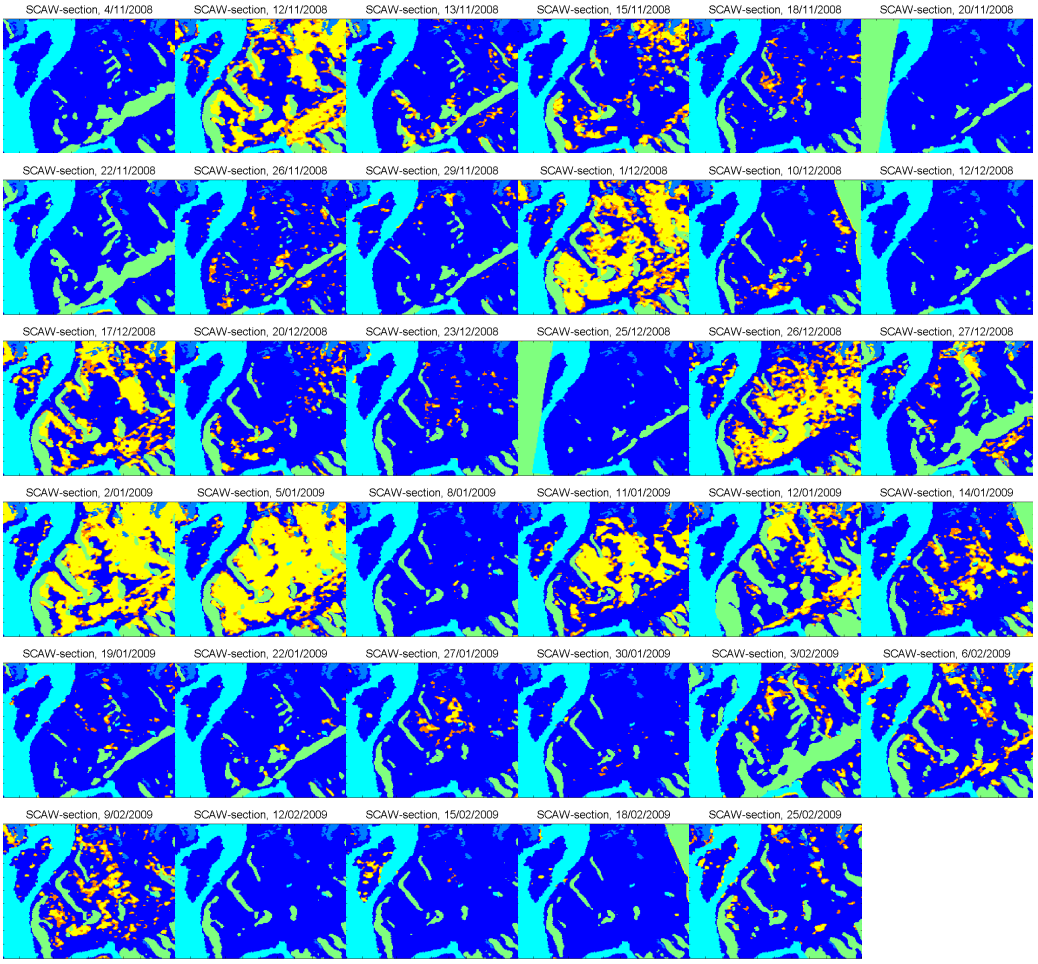

Figure 6.13: Timeserie of the 2008/2009 winter season from November 4th 2008 to February 25th 2009 for avalanche site 3. Yellom areas represent wet snow, orange areas represent possible wet snow, green areas are areas with no coverage, dark blue areas represent dry snow or land, blue areas are marshes, and light blue areas are ocean.

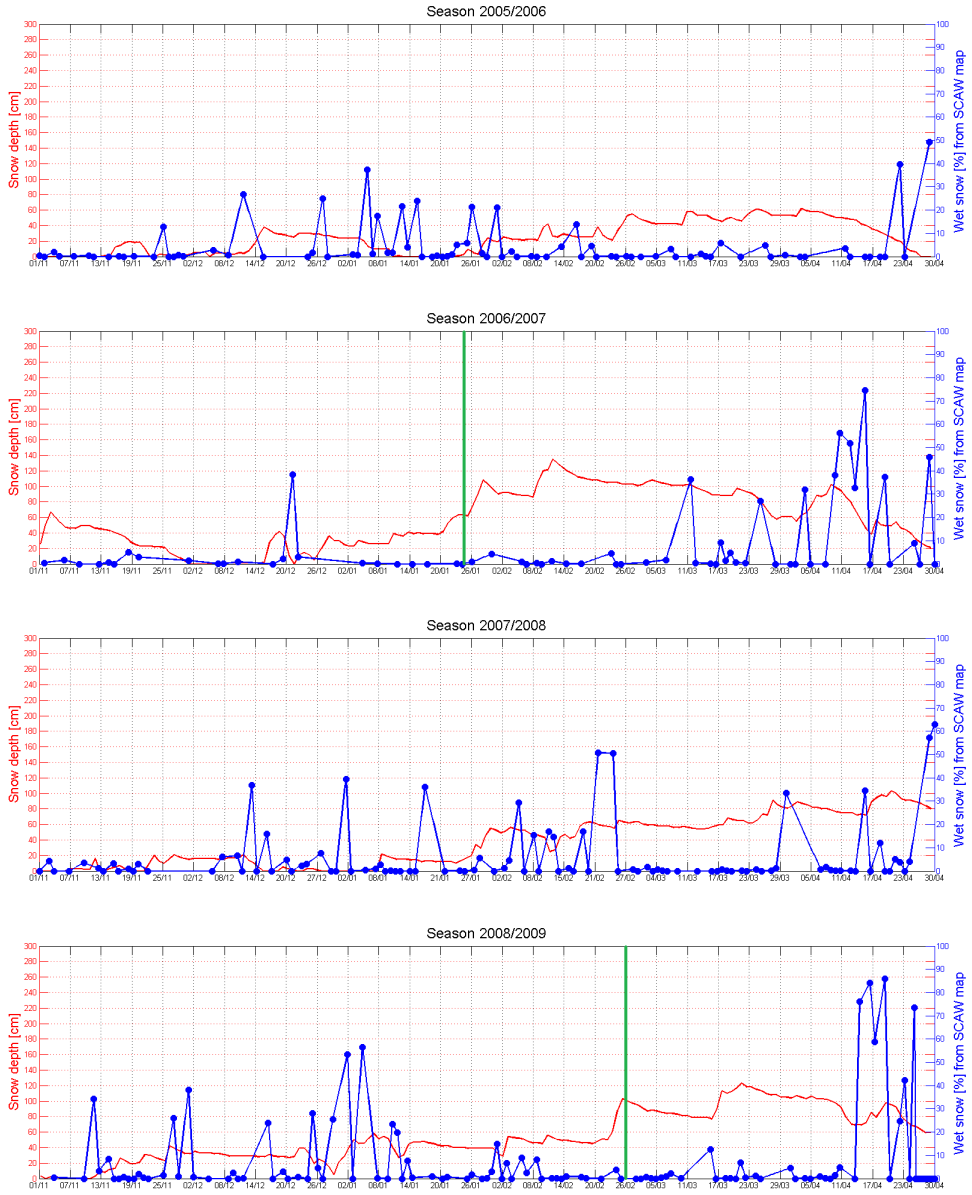

Figure 6.14: Detected wet snow fraction plot for avalanche site 3 for the winter seasons, starting with the 2005/2006 season in the top image, and ending with the 2008/2009 season in the bottom image. The green, vertical line in the second plot from the top marks the avalanche incident January 25th 2007. The green, vertical line in the last image marks the avalanche accident at Kroken, 26th February 2009. Method 1 is used as reference method. The blue dots mark the real values for the SCAW wet snow fraction. The blue line shows the interpolated values of the wet snow fraction, and the red line shows snow depth.

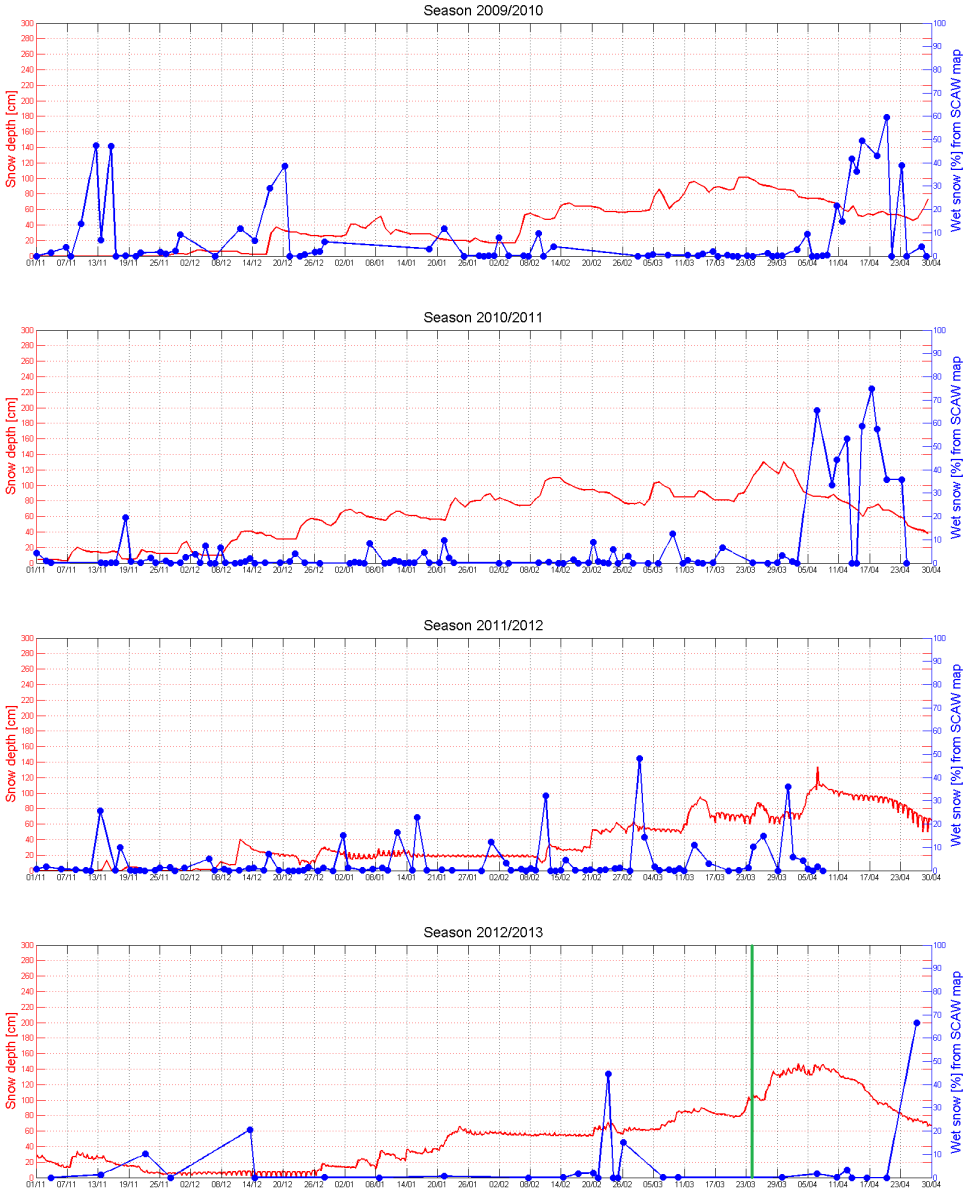

Figure 6.15: Detected wet snow fraction plot for avalanche site 3 for the winter seasons, starting with the 2009/2010 season in the top image, and ending with the 2012/2013 season in the bottom image. The green, vertical line in the last image marks the avalanche accident at Kroken, 24th March 2013. Method 1 is used as reference method. The blue dots mark the real values for the SCAW wet snow fraction. The blue line shows the interpolated values of the wet snow fraction, and the red line shows snow depth.

In the wet snow plot from the 2009/2010 season in Figure 6.18 we see some peaks in November and December. Then there are no indications of snowmelt until April. The 2010/2011 season show no snowmelt until April and the wet snow plot for 2011/2012 show no snowmelt of importance during the whole season. The wet snow fraction plot covering the 2011/2012 winter season in Figure 6.18, has only one small peak (approximately 15% wet snow of the total number of land pixels) a couple of weeks before the avalanche accident at Sorbmegaisa, March 19th 2012. A timeserie of SCAW maps covering the site from the start of the 2011/2012 winter season up to the avalanche accident, is shown in Figure 6.16.

The last plot in Figure 6.18 shows a small peak in the wet snow curve for the 2012/2013 season between February 20th and February 26th, but nothing more until April. An increase and decrease in the snow depth is seen between February 26th and March 4th. This indicates that there has been wet snow in this time period, but with the lack of SAR data for this season, it is difficult to know for sure.

The snow depth curves for Sorbmegaisa are based on weather data from Sørkjosen Airport, except for the 2005/2006 and 2006/2007 winter seasons, where the snow depth curves are based on data from Tromsø weather station.

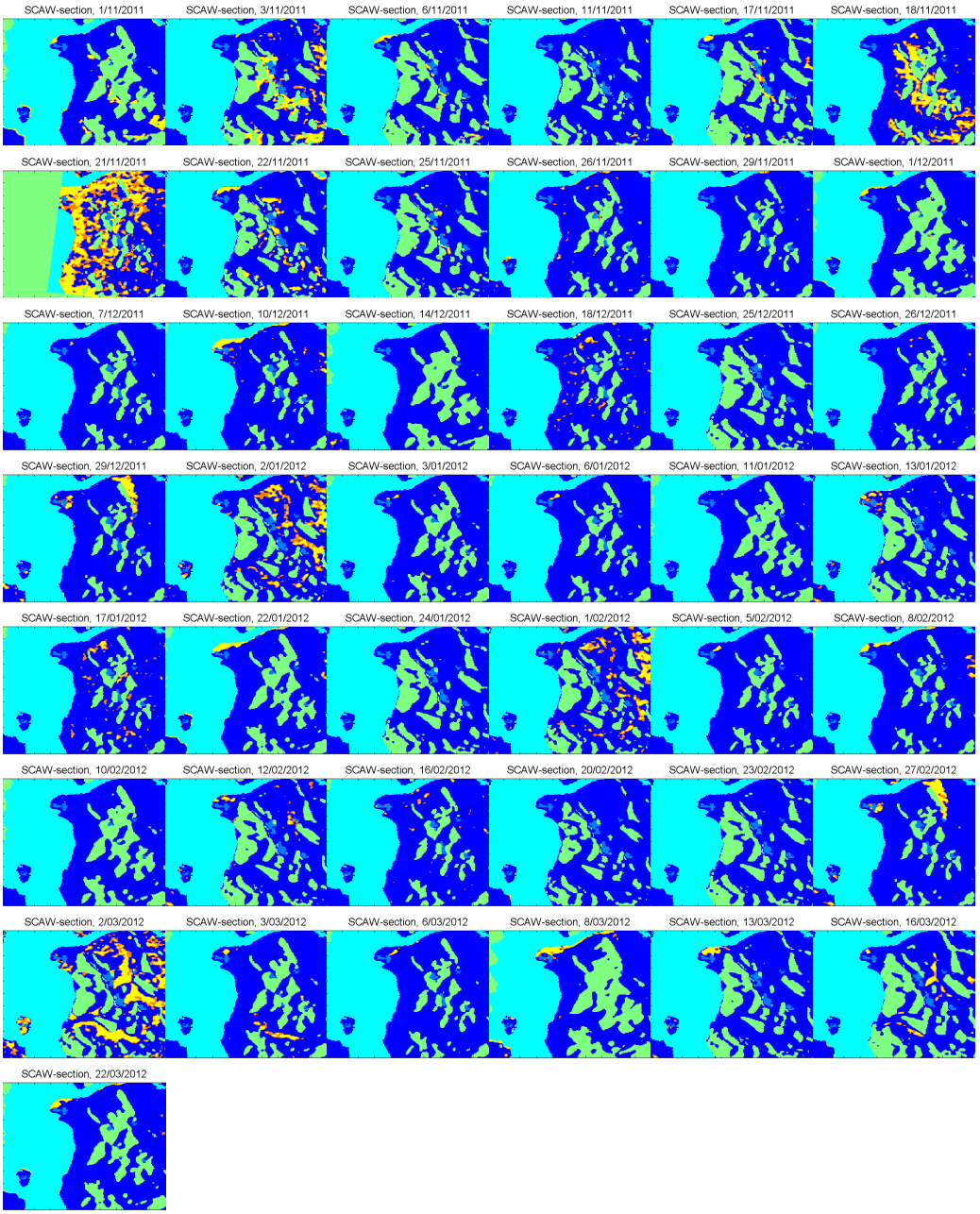

Figure 6.16: Timeserie of the 2011/2012 winter season from November 6th 2011 to March 22nd 2012 for avalanche site 4. Yellom areas represent wet snow, orange areas represent possible wet snow, green areas are areas with no coverage, dark blue areas represent dry snow or land, blue areas are marshes, and light blue areas are ocean.

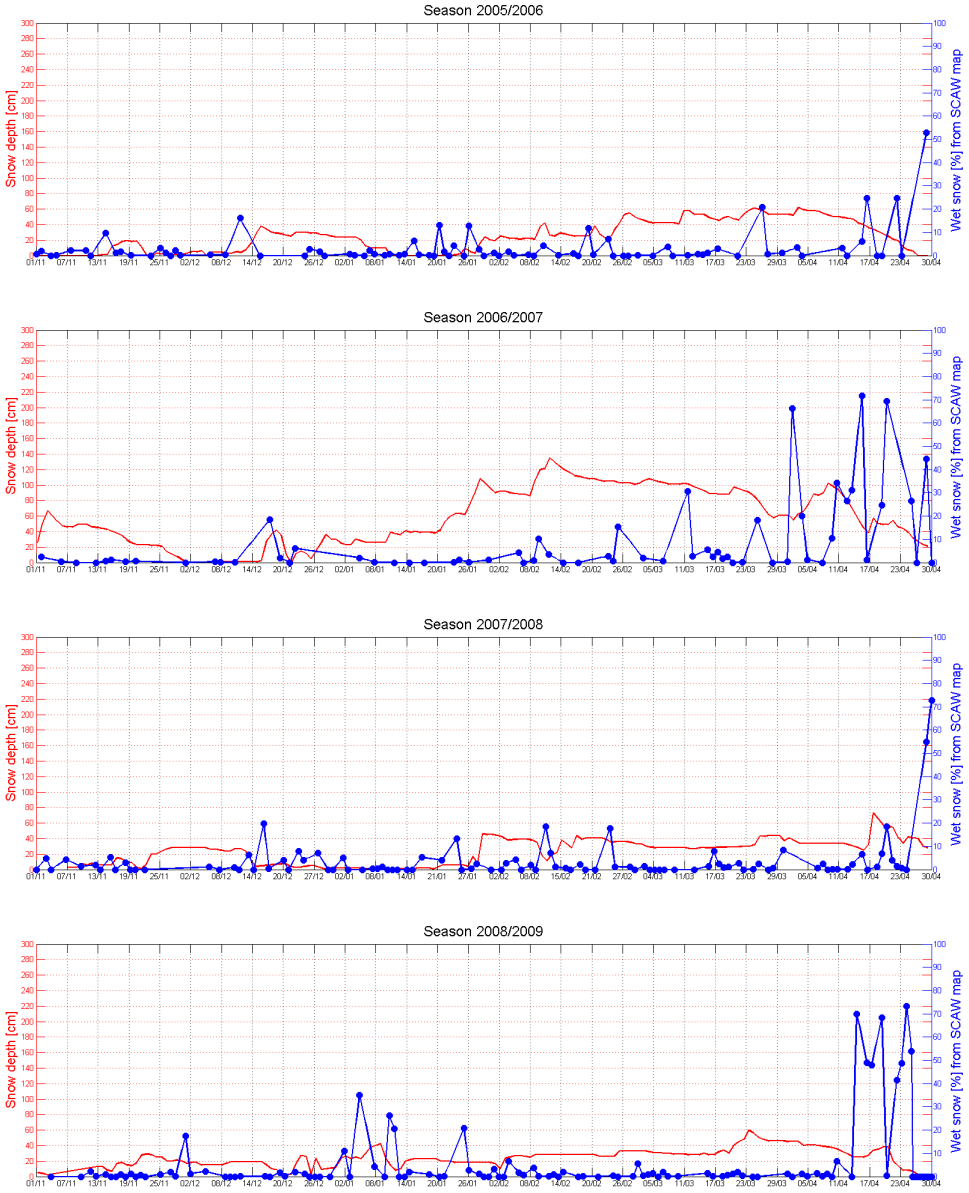

Figure 6.17: Detected wet snow fraction plot for avalanche site 4 for the winter seasons, starting with the 2005/2006 season in the top image, and ending with the 2008/2009 season in the bottom image. Method 1 is used as reference method. The blue dots mark the real values for the SCAW wet snow fraction. The blue line shows the interpolated values of the wet snow fraction, and the red line shows snow depth.

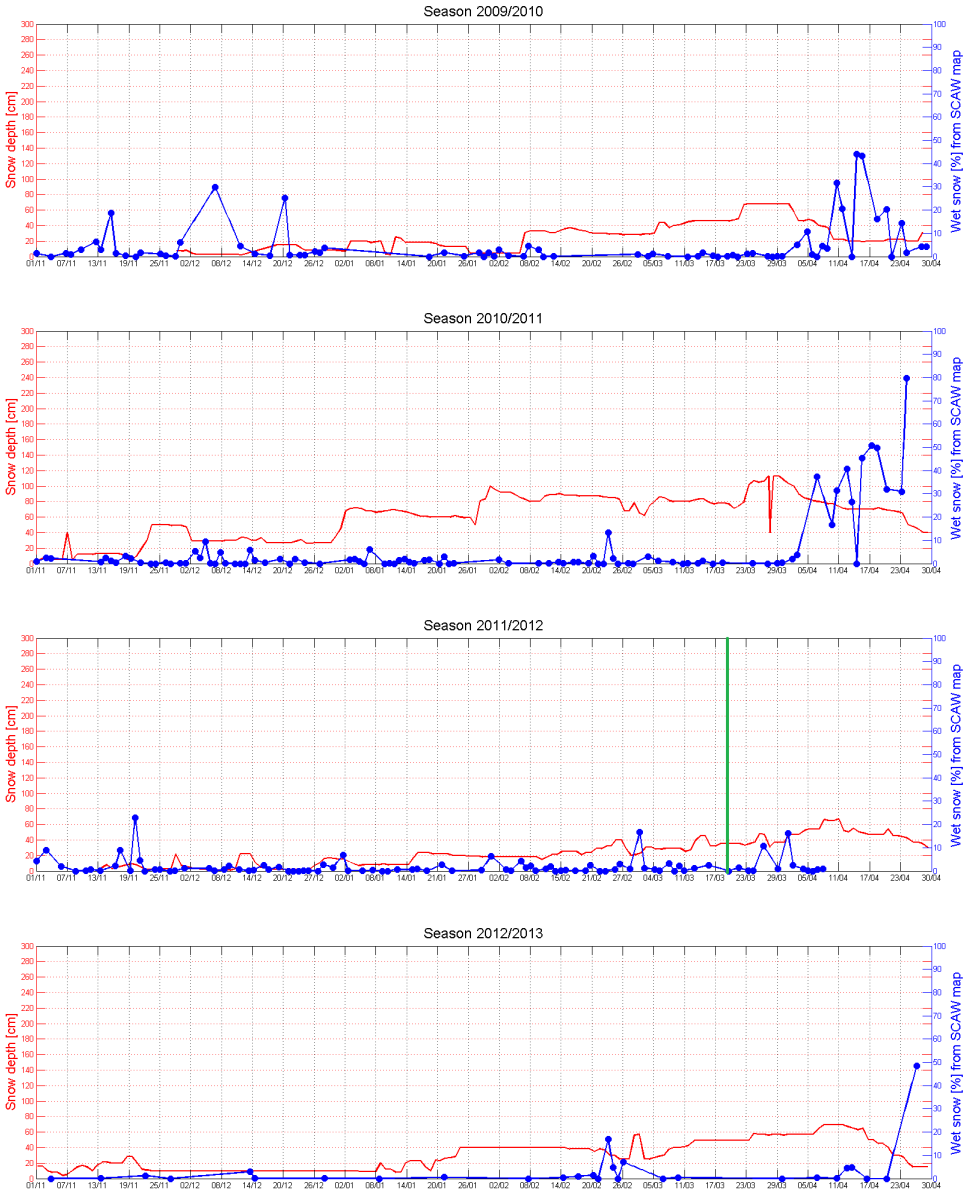

Figure 6.18: Detected wet snow fraction plot for avalanche site 4 for the winter seasons, starting with the 2009/2010 season in the top image, and ending with the 2012/2013 season in the bottom image. The green, vertical line in the second to last image marks the avalanche accident at Sorbmegaisa, 19th March 2012. Method 1 is used as reference method. The blue dots mark the real values for the SCAW wet snow fraction. The blue line shows the interpolated values of the wet snow fraction, and the red line shows snow depth.

Chapter 7

Discussion

7.1 Temperature maps

The temperature maps are calculated from the meteorological data from one weather station, located in Tromsø city, close to the coast of Troms county. The temperature of each pixel is based on an assumed lapse rate for temperature of 0.6°C per 100m (see Equations 5.1-5.3). This is a very coarse estimate, and does not apply under all conditions. Another simplification is the use of a single station situated close to the coast. The inland temperature of Troms can differ greatly from the coastal temperature, especially on days when low pressure systems are coming in from west, but have not yet reached the inland. This means that the temperature maps must be used more as guidance and not a blue print.

A better method for deriving these maps would be to use temperature data from multiple weather stations located in the area of the test site, and interpolated the temperature of each pixel using different weights based on the pixel's distance from the stations and the height above sea level of each pixel.

7.2 Reference methods

7.2.1 Method 1

Method 1 has the advantage that it is easy to use, and when using proper temperature thresholds, it is almost guaranteed that there will not be wet

snow in the reference image. The disadvantage is that there could be a difference in backscatter from the ground due to, e.g., variations in the wetness of the top layer. This could result in false detection of wet snow. Speckle could also be a problem, as the reference images are not averaged.

As seen in the wet snow fraction plot for method 1 for the 2006/2007 winter season, Figure 6.5, method 1 follows the temperature derived wet snow fraction curve quite well, even if the detected values are generally lower than the temperature derived ones. In November and December the temperature derived wet snow plot in Figure 6.5 indicates snowmelt, and so does the snow depth curve in the same figure. The detected wet snow fraction curve on the other hand, shows almost no signs of the presence of wet snow. This might have something to do with the fact that both the temperature and the snow depth is measured in Tromsø city, and does not necessarily apply for the rest of the test site. The detected wet snow curve in the top plot of Figure 6.5 also indicates snowmelt on times when the temperature derived plot does not show sign of snowmelt, seen around February 8th and February 26th 2007. The reason for this can be that wet snow that follows a warm period might not show up on the temperature derived plot, since the temperature derived wet snow fraction only takes into account pixels of more than 1°C.

7.2.2 Method 2

Method 2 has the advantage that images that are certain to contain dry snow are averaged. This result in speckle reduction and less erroneous wet snow detection, since the variations in backscatter due to variations on the ground are decreased. One disadvantage with this method is that five images is not always enough to average out the variations in backscatter, which means that there could still be incorrect detections of wet snow.

From Figure 6.4 it is possible to see that the standard deviation of the backscatter in the images that make up the reference images for method 2 is quite high, which suggest that the SAR data used to make the averaged reference images contains a lot of variations. This might be the reason for the lower amounts of detected wet snow compared to that of method 1, as seen in Figure 6.2 and Figure 6.1. Another reason for the lower detection could be that the averaged reference images help remove falsely detected wet snow, due to surface variations, which we may get in the wet snow maps produced with method 1.

7.2.3 Method 3

Method 3 has the advantage that many images are averaged to make the reference image. This results in high speckle reduction and more averaging of the backscatter variations that are not due to melting snow. A disadvantage of this method is that it is hard to separate out images that may contain wet snow, since the standard deviation method, explained in chapter 5, is quite coarse. This can result in less wet snow detected than there actually is.

The standard deviation of the backscatter in the reference images in method 3 is shown in Figure 6.4. Here we can see that before the outliers are removed, the variations within the reference images are large for some of the tracks. After removal of the outliers, the standard deviations are smaller, but they still indicate that there are some variations within the reference images.

The timeserie of wet snow maps made with method 3 in Figure 6.3 shows that method 3 has a lower wet snow detection than method 1. The only exception is the last image of the timeseries, where the method 3 map has the largest wet snow cover of all the methods. When comparing the two timeseries in Figure 6.2 and Figure 6.3, we see that method 2 and method 3 has almost the same amount of wet snow detection, but it looks like method 3 has a slightly higher detection rate than method 2. When comparing the wet snow fraction plots of method 3 in Figure 6.5, Figure 6.6, Figure **??**, and Figure **??** with the method 2 plots in the same figures, we find that method 3 has a higher detection rate of wet snow when the method covers the whole test site. When the focus is on the coastal region, method 2 has a higher detection rate. The coastal region will probably contain more snow than the rest of the test site, so the reference images of method 3 for this region may contain more wet snow and produce a lower wet snow detection than method 1 and method 2, which have temperature constraints on the SAR data used in the reference images. Another reason for the lower wet snow detection in the coastal parts could come from the use of a maximal mask in method 3, which is necessary because the SAR images from the same tracks are taken at slightly different locations, thus changing the layover and foreshortening geometry. When averaging all the images in a track, the mask has to cover all the different layover and foreshortening geometries. This makes the maximal mask for the tracks with a high number of images larger than for the other two methods that use only one or five images in the reference images. As the coastal areas have a higher concentration of steep mountains than the inner parts of the mainland, the maximal mask might contribute to the lower wet snow detection of method 3 for the coast.

7.2.4 Correlation plots

The two scatter plots to the left in Figure 6.9 agree with the observation of a generally lower amount of detected wet snow compared to the amounts of temperature derived wet snow. The scatter plot at the top left represents the whole test site, while the scatter plot at the bottom left represents the coastal region only. The plot covering the whole test site show a lower degree of correlation than the scatter plot covering the coastal parts. The higher values of wet snow for the coast are probably the result of higher temperatures in the land areas close to the coastline, which is normal for the Norwegian climate.

The two scatter plots of method 2 are shown in the middle part of Figure 6.9. They display a lower degree of correlation than the scatter plots of method 1. We get a worse correlation for method 2 because method 2 has a lower detection rate of wet snow than method 1.

The scatter plots from method 3, shown in the right part of Figure **??**, indicates that the correlation between the temperature derived wet snow fraction values and the detected ones is better for method 3 than for method 2 when we look at the whole test site, but when it comes to the coastal region scatter plot, the correlation between the two methods seems equally bad.

The plots shown in Figure 6.9 do not yield an unambiguous answer. Most of the data points lie along or close to the y-axis. This is probably due to the fact that the detected wet snow fraction values are lower than the temperature derived wet snow fraction values for the three methods. One reason for the lower values is discussed in the beginning of this chapter. Few of the scatter points lie along the ideal correlation line. The scatter plots in the bottom part of Figure 6.9 show that removing the mainland parts and keeping the coastal parts gives higher values of detected wet snow, as some of the scatter points have moved away from the y-axis. Still, there is no clearly visible correlation shown in the plots, but the correlation plot from method 1 appears to have fewer scatter points along the y-axis, when compared to the other plots.

7.2.5 The preferred reference method

Based on the findings of section 7.2, I chose in the following to work with reference method 1, as it seems to be the one with the highest detection of wet snow. I am not sure if this is the more correct method, as I have no in situ

data to control my findings, but compared to the temperature derived wet snow fraction plots, method 1 seems to have a higher correlation than method 2 and 3. Besides, as the main hypothesis of this paper is to investigate the relationship between melting and freezing cycles and avalanches, I find that it is better to have higher wet snow detection, so that cycles are highlighted during the winter seasons.

7.3 Relation between wet snow and avalanches

7.3.1 Avalanche site 1 and 2

On February 19th 2006, a skier was taken by an avalanche on Middagstinden. A timeserie of SCAW maps for the 2005/2006 winter season up to the avalanche accident, is shown in Figure 6.10. The last image in the timeserie is taken the day after the avalanche event. Looking at the timeserie of the 2005/2006 winter season, we see indications of a large amount of melting snow late in December, early in January, in the middle of January, late in January, and early in February. The same signs of melting snow is shown in the wet snow fraction plot for the 2005/2006 season in Figure 6.11. Examining the snow depth shown as a red line in the same plot, we find that there indeed was a decrease in snow depth during the periods of indicated melting. Figure 6.11 also shows that there was a similar melting pattern in the 2008/2009 winter season, with large amount of melting snow in the first half of January, but with a slightly smaller amount of melting snow in the beginning of February, only here the snow depth seems to be increasing during some of the indicated melting periods, as seen in the beginning of January and end of February.

On February 18th, 2012, four men were taken by an avalanche on Middagstinden. Two managed to get out, two died. A wet snow fraction plot of the 2011/2012 season, amongst other, is shown in Figure 6.12. Studying the snow depth and wet snow plot for the 2011/2012 season in Figure 6.12, we see that the snow depth was quite stable from early January to the middle of February, and that the wet snow fraction curve indicates presence of wet snow just after February 8th. We also see a dip in the snow depth curve around that time.

In March 2013, one man was killed by an avalanche on Langfjellaksla. A wet snow fraction plot of the 2012/2013 winter season, amongst other, is shown in Figure 6.12. Due to the lack of SAR data for this season, there are only

a few values of detected wet snow in the plot. The wet snow fraction value between February 20th and February 26th exceeds 60%, which is unusually high this early in the winter season.

7.3.2 Avalanche site 3

On January 25th 2007, two skiers were taken by an avalanche in Kroken Alpine Center, but both survived. In the wet snow fraction plot from the 2006/2007 winter season shown in Figure 6.14, there is almost no detected snowmelt early in the season, except for one peak around December 20th 2006, which also can be seen in the decrease in snow depth around that date. In the 2007/2008 plot, we see indications of large amounts of melting snow in the second half of February, but this is not evident when looking at the snow depth curve.

On February 26th 2009, a woman lost her life in an avalanche accident in the alpine center. A timeserie of SCAW maps covering the area for the 2008/2009 winter season up to the day of the accident, is shown in Figure 6.13, and a wet snow fraction plot over the season is shown in Figure 6.14. Figure 6.13 shows that snowmelting was detected early in December and early in January in the 2008/2009 season, which is also seen in the last plot in Figure 6.14. The snow depth curve in the same plot also indicates snowmelting in the end of December and the start of January.

On March 24th 2013, a man was killed in approximately the same area as the person in 2009. A wet snow fraction plot over the 2012/2013 winter season is shown in Figure 6.15. In Figure 6.15, there are no clear indications of melting snow, except late in December 2009, and a high peak late in February 2013. Even so, the small amounts of detected wet snow and the fluctuations in the snow depth curve seem to coincide. The snow depth seems unaffected by the high peak in detected wet snow in February 2013.

7.3.3 Avalanche site 4

Avalanche site 4 is located in Kåfjorden, and covers Sorbmegaisa and surrounding areas. Sorbmegaisa was the scene of a large avalanche accident on March 19th, 2012, where five ski tourists were killed. A timeserie of SCAW maps covering the site is shown in Figure 6.16, and a wet snow fraction plot of the 2011/2012 season is shown in Figure 6.18. Figure 6.16 shows little to no detected snowmelt in the time period before the avalanche accident in

March. There is a small amount of melting around March 2nd in the higher areas. Almost none of the wet snow fraction plots in figures 6.17 and 6.18 show any early to mid-season snowmelt, except in January 2009, where we also find a reduction in snow depth. In the 2012/2013 season, shown in the bottom plot in Figure 6.18, the little detected snow data we have indicates the presence of wet snow late in February. The snow depth curve has rapid increase and a just as rapid decrease in the same time period.

There seems to be a tendency for the wet snow fraction plots for avalanche site 4, seen in figures 6.17 and 6.18, to have lower values of detected wet snow than the wet snow fraction plots for the other avalanche sites. The reason for this is probably that most of the area this site covers lies on higher elevations than the areas covered by the other avalanche sites. It is possible to recognize the warm periods that cause high detection rates in the wet snow fraction plots in the previous sections, but the peaks in the wet snow fraction plots for avalanche site 4 are a lot lower than those seen in the plots from avalanche site 1, 2, and 3.

7.3.4 Avalanche data findings

It is hard to find anything to indicate whether or not the melt periods stabilize or destabilize the snowpack. We have one season, 2008/2009, with a lot of snowmelt early in the season prior to an avalanche incident (Kroken, February 29th 2009). The same system can be found in the plots from 2005/2006 preceding an avalanche event (Middagstinden February 19th 2006), but we can also find a similar pattern in 2007/2008, and in the plots from 2009/2010, without any avalanches being released in the avalanche areas I focus on. Then again, with all the avalanche accidents I am studying being triggered by humans, the conditions in the 2007/2008 and 2008/2009 seasons could have been just as unstable as the ones in the 2005/2006 and 2008/2009 seasons, there were just nobody there to trigger the avalanches.

The Tromsø region experienced many avalanches during the 2012/2013 season. Wet snow fraction plots from that season, seen in Figure 6.12 and Figure 6.15 show a wet snow cover of 60% for Kattfjordeidet and over 40% for Kroken Alpine Center between February 20th and February 26th, and the snow depth curve shows that snow fell after the snowmelt. Both these sites were sites of two fatal accidents that season. The avalanche reports for the accidents states that both the avalanches slid on a crust buried under a layer of snow [22]. A crust that probably formed during the snowmelt in the end of February.

If our assumption is that melting and freezing destabilizes the snowpack by forming a sliding bed for an avalanche, it is essential for a certain amount of snow to fall on top of the melt/freeze crust. If there is no snow on top of the crust, then there is no snow to slide on the crust either, and thus, no avalanche. When studying the wet snow fraction plots of the avalanche accidents at Kroken Alpine Center, shown in Figures 6.14 and 6.15, I find that they all have a high degree of melting approximately one to one and a half months before the avalanche events, and an increase in snow depth just before the avalanche. This could mean that the avalanches were sliding on a crust formed during the melting one month earlier. One other thing that seems to have an impact on the snow stability, is the fact that the high peaks seem to be followed by little to no detected wet snow until the avalanches are triggered. This indicates that the wet snow period was succeeded by a cold period, which could mean that the melt/freeze crust formed before the snow that fell afterwards was able to bond with the old snow layer.

From the situations described above, one could form the hypothesis that high amounts of wet snow combined with a snow layer deep enough not to melt completely away, can form a crust that will become a weak layer if enough snow falls on top of the crust and the snow is unable to bond with the crust.

A problem with this hypothesis is the fact that avalanches are products of multiple different factors, like wind direction and velocity, the amount of precipitation, the temperature of the area in question, etc. Some season there is more snowmelting before an avalanche incident, and some seasons there is little. It might be that the effect of melting changes with different weather circumstances, working to stabilize the snowpack if the snowpack already is layered, or destabilizing it if the melting is followed by a large snowfall and cold weather.

Chapter 8

Conclusion

This thesis had two different objects: one object was to find the best method for making reference images to use in the wet snow detection algorithm, and one object was to investigate if melting and freezing of snow in early winter and/or mid-winter would make the snowpack become more stable or less stable.

The best reference method was found by making wet snow fraction plots based on the amount of detected snowmelt and comparing the plots to wet snow fraction plots based on the number of land pixels with a temperature value above 1°C. Scatter plots were made to make any correlation between the detected wet snow fraction data and the temperature derived data more evident. Wet snow fraction plots were made for the coastal region of the site, in an attempt to get a better correlation between the temperature derived wet snow fraction plots and the detected wet snow fraction plots.

To investigate the effect of snowmelt on snow stability, wet snow fraction plots that focused on the scene of the avalanches, were made. For some of the avalanche incidents, timeseries of detected wet snow maps (SCAW maps) covering the same areas as the wet snow fraction plots, were made. These showed the distribution of wet snow during a season up to the avalanche was triggered. Snow height measurements from Tromsø and Sørkjosen Lufthavn were plotted together with the wet snow fraction curves.

After examining the wet snow fraction plots for the different avalanche scenes, one pattern stood out, as four out of the seven avalanche events I studied appear to follow this pattern. The characteristics of the pattern are listed as follows:

- There has to be a significant amount of wet snow
- The snow has to be deep enough not to melt away
- New snow must fall after the snowmelt
- The snowmelt has to be followed by a cold period

As an end note I just want to point out that to single out one factor out of a hundred and then try do predict future based on knowledge of only that one factor, is basically impossible. And not what I set out to do. The hope was to find a correlation between the different patterns of snowmelt before an avalanche incident, and thus to show that this method of detecting wet snow by satellite can contribute to the avalanche forecasting which is already established in Norway. I do not believe that a have found a correlation that will be able to predict avalanches if used by itself, but maybe, if used together with the already established methods of avalanche forecasting, could be a useful tool.

8.1 Future work

There are some things that could have been done to increase the accuracy of the findings in this thesis. Better temperature maps would improve the temperature derived wet snow plots, which again could improve the correlation between the temperature derived wet snow fraction and the detected wet snow fraction.

The prevalence in height of the detected wet snow is an issue I have not considered in my wet snow fraction plots. If melting occurred on high elevation it would probably have a higher impact on the snowpack stability than melting on lower elevations. A DEM could be used to separate wet snow detected under a height threshold from wet snow detected above the same threshold. The wet snow detected above the threshold would probably be more important for the snowpack stability than the wet snow under.

Having more detailed knowledge of avalanche events would be helpful, and this will be achievable now as the avalanche forecasting in Norway has started to gather avalanche observations in an open database.

On a larger perspective, many interesting things are happening in the field of remote sensing of snow, something the CoreH20-report (2012) is an example of. This report focuses on the possibilities of a satellite that operates in the

X- og Ku-band, which will give the satellite the ability to measure the extent and mass of the seasonal snow cover. This kind of data can be extremely helpful when it comes to avalanche forecasting. Knowledge about snow depth, grain structure, and layering of the snowpack is also important in avalanche forecasting. Solberg et al. (2010) show how optical remote sensing can give us information about these snow parameters. Thus, a combination of SAR and optical sensor could be very useful as an aid in avalanche forecasting.

References

[1] Armstrong, R.L. and Brodzik, M.J., (2001) "Recent Northern Hemisphere Snow Extent: A Comparison of Data Derived from Visible and Microwave Satellite Sensors" *Geophysical Research Letters*, Vol. 28, No. 19, pp. 3673-3676

[2] Baghdadi, N.,Gauthier, Y. and Bernier, M. (1997) "Capability of Multitemporal ERS-1 SAR Data for Wet-Snow Mapping" *Remote Sensing of the Environment*, Vol. 60, No. 2, pp. 174-186

[3] Birk, R., Camus, W. and Valenti, E. (1995) "Synthetic Aperture Radar Imaging Systems" *Aerospace and Electronic Systems Magazine, IEEE*, Vol. 10, No. 11, pp. 15-23

[4] Brown, W. M. and Porcello, L. J. (1969) "An introduction to synthetic-aperture radar" *Spectrum, IEEE*, Vol. 6, No. 9, pp. 52-62

[5] Chan, Y.K. and Koo, C. (2008) "An introduction to synthetic aperture radar (SAR)" *Progress In Electromagnetics Research B*, Vol. 2, pp. 27-60

[6] Chuvieco, E. and Huete, A. (2010) "Fundamentals of satellite remote sensing". Boca Raton, FLA: CRC Press

[7] Report for Mission Selection: $CoReH_2O$, ESA SP-1324/2 (3 volume series), European Space Agency, Noordwijk, The Netherlands

[8] Cumming, W. A. (1952) "The dielectric properties of ice and snow at 3.2 centimeters" *Journal of Applied Physics*, Vol. 23, No. 7, pp. 768-773

[9] Fritzsche, H., Phillips, M., "Electromagnetic radiation" *Encyclopædia Britannica*, 2007, *Britannica Online*, Web, Retreived 20th May 2013

[10] Elachi, C. and Zyl, J. van (2006) "Introduction to the physics and techniques of remote sensing", 2nd edition. Hoboken, New Jersey: John Wiley & Sons, Inc.

[11] www.eklima.no

[12] "ESA declares end of mission for Envisat" (n.d.) *ESA* Retrieved November 13th, 2013

[13] Foster, J. L., Hall, D. K., Chang, A. T. C. (1984) "An Overview of Passive Microwave Snow Research and Results" *Reviews of Geophysics and Space physics*, Vol. 22, No. 2, pp. 195-208

[14] Hallikainen, M., Ulaby, F. T., and Abdelrazik, M., (1986) "Dielectric properties of snow in the 3- to 37-GHz range" *IEEE Transactions on antennas and propagations*, Vol. AP-34, No. 11, pp.1329-1340

[15] Lauknes, I. and Malnes E. (2004) "Automatical geocoding of Envisat ASAR products" *ESA Envisat & ERS Symposium*, Salzburg, Austria

[16] Lied, K. and Kristensen, K., (2003) "Snøskred. Håndbok om snøskred". Nesbru, Norway: Vett & Viten AS

[17] Koskinen, J. T., Pulliainen, J. T., and Hallikainen, M. T. (1997) "The use of ERS-1 SAR data in snow melt monitoring" *ransactions on geoscience and remote sensing, IEEE*, Vol. 35, No. 3, pp. 601-610

[18] König, M., Winther, J-G., Isaksson, E. (2001) "Measuring snow and ice properties from satellite" *Reviews of Geophysics*, Vol. 39, No. 1, pp. 1-27

[19] Male, D.H. (1980) "The seasonal snowcover" *Dynamics of snow and ice masses*, pp. 305-395. Editor: Samuel C. Colbeck, New York, New York: Academic Press

[20] Meier, M. (1975) "Application of remote-sensing techniques to the study of seasonal snow cover" *Journal of Glaciology*, Vol.15, No. 73, pp. 251-265

[21] Nagler, T. and Rott, H. (2000) "Retrieval of Wet Snow by Means of Multitemporal SAR Data" *Transactions on geoscience and remote sensing, IEEE*, Vol. 38, No. 2, pp. 754-765

[22] "Ulykker" (n.d.) *snoskred.no* Retrieved November 14th, 2013

[23] Anna W. Nolin (2010) "Recent advances in remote sensing of seasonal snow" *Journal of Glaciology*, Vol. 56, No. 200, pp. 1141-1150

[24] Norwegian Water Resources and Energy Department (2013) "Snøskredvarslingen i Norge" *Norges vassdrag- og energidirektorat*, Retreived July 12, 2013 from *www.nve.no*

[25] Rees, W.G. (2006) "Remote sensing of snow and ice". Boca Raton, Florida: Taylor & Francis Group

[26] Robinson, D. A., Dewey, K. F., Heim Jr., R. R., (1993) "Global Snow Cover Monitoring: An Update" *Bulletin of the American Meteorological Society*, Vol. 74, No. 9, pp. 1689-1696

[27] Rott, H. (1984) "The analysis of backscattering properties from SAR data of mountain regions" *Journal of oceanic engineering, IEEE*, Vol. OE-9, No. 5, pp. 347-355

[28] Rott, H. and Matzler, C (1987) "Possibilities and limits of synthetic aperture radar for snow and glacier surveying" *Annals of Glaciology*, Vol. 9, pp. 195-199

[29] Shi, J. (2008) "Active Microwave Remote Sensing Systems and Applications to Snow Monitoring" *Advances in Land Remote Sensing*, pp. 19-49. Editor: Liand, S., Netherlands: Springer Netherlands

[30] Shi, J. and Dozier, J. (1992) "Radar backscattering response to wet snow" *Geoscience and Remote Sensing Symposium, 1992. IGARSS '92. International*, Vol. 2, pp. 927-929

[31] Shi, J., Dozier, J. and Rott, H. (1994) "Snow Mapping in Alpine Regions with Synthetic Aperture Radar" *Transactions on geoscience and remote sensing, IEEE*, Vol. 32, No. 1, pp. 152-158

[32] Solberg, R., Koren, H., and Wangensteen, B. (2010) "Remote sensing of snow characteristics for avalanche warning" *"Snøskred" project results from 2008-2009*, SAMBA/09/10

[33] Stiles, W. H. and Ulaby, F. T. (1980) "The Active and Passive Microwave Response to Snow Parameters, 1. Wetness" *Journal of Geophysical Research*, Vol. 85, No. C2, pp. 1037-1044

[34] Stiles, W. H. and Ulaby, F. T. (1981) "Dielectric properties of snow" *Remote Sensing Laboratory*, RSL Technical Report 527-1

[35] Tremper, B. "Staying alive in avalanche terrain", 2nd edition. Seattle, Washington: The Mountaineers Books